

# Improved Connection Details for Adjacent Prestressed Bridge Beams

Final Report  
March 2015

**Carin Roberts-Wollmann**  
Professor  
Virginia Tech  
Blacksburg VA 24061

**Tommy Cousins**  
Professor  
Virginia Tech  
Blacksburg VA 24061

**Kedar Halbe**  
Graduate Research Assistant  
Virginia Tech  
Blacksburg VA 24061

**Carrie Field**  
Graduate Research Assistant  
Virginia Tech  
Blacksburg VA 24061

External Project Manager  
Michael Brown, Ph.D., P.E.  
Research Project Manager  
Virginia Center for Transportation Innovation and Research

In cooperation with  
Rutgers, The State University of New Jersey  
And  
State of Virginia  
Department of Transportation  
And  
U.S. Department of Transportation  
Federal Highway Administration

## **Disclaimer Statement**

The contents of this report reflect the views of the authors, who are responsible for the facts and the accuracy of the information presented herein. This document is disseminated under the sponsorship of the Department of Transportation, University Transportation Centers Program, in the interest of information exchange. The U.S. Government assumes no liability for the contents or use thereof.

TECHNICAL REPORT STANDARD TITLE PAGE

1. Report No. CAIT-UTC-001	2. Government Accession No.		3. Recipient's Catalog No.	
4. Title and Subtitle  Improved Connection Details for Adjacent Prestressed Bridge Beams			5. Report Date March 2015	
			6. Performing Organization Code CAIT/Virginia Tech	
7. Author(s) Carin Roberts-Wollmann, Thomas Cousins, Kedar Halbe, Carrie Field			8. Performing Organization Report No. CAIT-UTC-001	
9. Performing Organization, Name and Address Department of Civil and Environmental Engineering Virginia Tech 200 Patton Hall Blacksburg, VA 24061			10. Work Unit No.	
			11. Contract or Grant No.  DTRT12-G-UTC16	
12. Sponsoring Agency Name and Address Center for Advanced Infrastructure and Transportation Rutgers, The State University of New Jersey 100 Brett Road Piscataway, NJ 08854			13. Type of Report and Period Covered Final Report 5/30/12 - 12/31/2013	
			14. Sponsoring Agency Code	
15. Supplementary Notes U.S Department of Transportation/Research and Innovative Technology Administration 1200 New Jersey Avenue, SE Washington, DC 20590-0001				
16. Abstract Bridges with adjacent box beams and voided slabs are simply and rapidly constructed, and are well suited to short to medium spans. The traditional connection between the adjacent members is a shear key filled with a conventional non-shrink grout. With time and traffic, many of the joints show signs of cracking and leaking, and eventually, corrosion of the reinforcing and prestressing steel within the beams. The overarching goal of this project was to develop an improved detail for the connection between adjacent members using Ultra-High Performance Concrete (UHPC) or Very High Performance Concrete (VHPC). The specific objective of the research presented in this report was to determine the appropriate splice length for No. 4 and No. 6 uncoated reinforcing bars used in a UHPC or VHPC connection. A total of 15 beams were tested to determine the appropriate splice lengths for uncoated No. 4 and No. 6 bars in UHPC and VHPC. The 12 in tall by 10 in wide by 8.5 ft beams were precast with conventional concrete, with a block-out pocket to accommodate a splice. The tension bars were spliced in the pocket, which was then filled with either VHPC or UHPC. The beams were tested to place the splice location in a region of constant moment, and were loaded monotonically to failure. It was found that for an uncoated No. 4 bar in UHPC or VHPC a splice length of 4 in is adequate to develop the yield strength of the bar, but a length of 5 in is recommended to insure ductility. For a No. 6 bar in UHPC a splice length of 5 in is adequate to develop the yield strength, but 6 in is recommended to insure ductility.				
17. Key Words Prestressed concrete box beams, connections, splice lengths, UHPC, VHPC			18. Distributional Statement	
19. Security Classification Unclassified	20. Security Classification (of this page) Unclassified	21. No. of Pages 71	22. Price	

## **Acknowledgments**

Funding for this project was provided by the Virginia Center for Transportation Innovation and Research (VCTIR) and the Tier I University Transportation Center Consortium led by CAIT at Rutgers University. The material contributions from Elkem, Titan America, and Bekaert are also gratefully acknowledged. Finally, the researchers would also like to thank Dennis Huffmann, Brett Farmer and Dr. David Mokarem for their support in the laboratory. The efforts of Hannah Crone, Mark Maguire and Doug Nelson were instrumental in the development of the VHPC mix, and are gratefully acknowledged. The guidance and technical assistance provided by the engineers at VCTIR and VDOT, including Dr. Mike Brown and Andy Zickler are also gratefully acknowledged. The opinions expressed in this report are those of the authors and not necessarily those of the sponsors.

## Table of Contents

1. INTRODUCTION .....	1
1.1. Adjacent Precast Member Connections .....	1
1.2. Ultra-High Performance Concrete Connections .....	1
1.3. Connection Testing Program.....	2
2. PURPOSE AND SCOPE.....	2
3. METHODS .....	3
3.1. Specimen Details.....	3
3.2. Test Setup.....	8
3.3. Test Procedure.....	9
3.4. Material Properties .....	10
4. RESULTS .....	11
4.1. Material Properties .....	11
4.1.1. Concrete Properties.....	11
4.1.2. Reinforcing Properties .....	12
4.1.3. Splice Pocket Filler Properties.....	15
4.2. Splice Test Results for No. 4 Bars and UHPC and VHPC Splice Pocket Filler .....	22
4.2.1. Summary of Test Results .....	22
4.2.2. Load vs. Displacement.....	24
4.2.3. Load vs. Strain .....	26
4.2.4. Load vs. Interface Opening.....	28
4.2.5. Load vs. DEMEC Strain Measurements .....	30
4.2.6. Crack Patterns and Failure Modes .....	31
4.3. Splice Test Results with No. 6 Bars and UHPC Splice Pocket Filler .....	38
4.3.1. Summary of Test Results .....	38
4.3.2. Load vs. Deflection.....	39
4.3.3. Load vs. Strain .....	41
4.3.4. Load vs. Interface Opening.....	42
4.3.5. Load vs. DEMEC Strain Measurements .....	44
4.3.6. Crack Patterns and Failure Modes .....	45
5. DISCUSSION.....	47
5.1. Summary of Strains in Compression Reinforcement.....	47

5.2. Strain Compatibility Analysis .....	48
6. CONCLUSIONS .....	56
7. REFERENCES .....	56
8. APPENDIX .....	58

## List of Figures

Figure 1. Adjacent Box Beam Connection with Drop-In Splice Bar .....	2
Figure 2. Typical Details of Initial Test Specimens .....	5
Figure 3. Typical Details of Modified Test Specimens .....	6
Figure 4. Typical Details of VHPC Test Specimens .....	7
Figure 5. Beam Mechanics: Tension Equals Compression for Equilibrium .....	8
Figure 6. Test Setup .....	9
Figure 7. Dog Bone Test Setup.....	11
Figure 8. Stress vs. Strain Plot for No. 4 Bars .....	13
Figure 9. Stress vs. Strain Plot for No. 6 Bars .....	14
Figure 10. Stress vs. Strain Plot for No. 7 Bars .....	14
Figure 11. Stress vs. Strain Plot for No. 8 Bars .....	15
Figure 12. Flexural Beam Test Results for VHPC at 7 Days .....	17
Figure 13. Typical 7 Day Flexural Beam Test Results for Untreated UHPC.....	18
Figure 14. VHPC Dog Bone Test .....	18
Figure 15. UHPC Dog Bone Test .....	19
Figure 16. Cracking Behavior of VHPC Dog Bone Sample 2 .....	20
Figure 17. UHPC Cracking Behavior .....	21
Figure 18. Comparison of VHPC and UHPC Dog Bone Specimens with 0.05 in Cracks .....	22
Figure 19. Load vs. South End Deflection for All Specimens with No. 4 Bars .....	25
Figure 20. Load vs. North End Deflection for Specimens with No. 4 Bars .....	25
Figure 21. Load vs. Midspan Deflection for Specimens with No. 4 Bars .....	26
Figure 22. Load vs. Reinforcement Bar (East) Strain for Specimens with No.4 Bars .....	27
Figure 23. Load vs. Reinforcement Bar (West) Strain for Specimens with No. 4 Bars .....	27
Figure 24. Force in Compressive Reinforcement from Externally Applied Loads .....	28
Figure 25. Schematic Representation of Cracks in the Precast Element Under the UHPC Pocket .....	29
Figure 26. Load vs. North Interface Displacement for Specimens with No. 4 Bars .....	29
Figure 27. Load vs. South Interface Displacement for Specimens with No.4 Bars .....	30
Figure 28. Locations and Designations of Locating Discs for DEMEC Gauge .....	31
Figure 29. DEMEC Strain Measurements at the Top of the Beam for Specimen U-4-5-I-E.....	31
Figure 30. UHPC Pocket in Specimen U-4-5-I-E Showing Interface Separation and Flexural Cracks .....	32

Figure 31. UHPC Pocket in Specimen U-4-6-I-E at End of Load Application Showing Flexural Cracks .....	32
Figure 32. UHPC Pocket in Specimen U-4-3-I Showing Cracks Near the Interfaces and the Corners .....	33
Figure 33. UHPC Pocket in Specimen U-4-5-II After Failure Showing South Interface Separation .....	33
Figure 34. Side View of UHPC Pocket in Specimen U-4-4-I After Failure Showing Interface Separation .....	34
Figure 35. VHPC Pocket in Specimen V-4-5-I Showing Interface Separation and Splitting Cracks .....	34
Figure 36. VHPC Pocket in Specimen V-4-6-I Showing Interface Separation and Splitting Cracks .....	35
Figure 37. VHPC Pocket in Specimen V-4-5-II Showing Interface Separation and Reinforcing Bars Ruptured .....	35
Figure 38. Specimen V-4-5-II at End of Load Application Showing the Reinforcing Bars Ruptured .....	36
Figure 39. VHPC Pocket in Specimen V-4-4-II Showing Interface Separation and Splitting Cracks .....	36
Figure 40. VHPC Pocket in Specimen V-4-3-I at End of Load Application Showing Interface Separation .....	37
Figure 41. VHPC Pocket in Specimen V-4-4-I at End of Load Application Showing Interface Separation .....	37
Figure 42. Load vs. South Deflection for All Specimens with No. 6 Bars.....	39
Figure 43. Load vs. North Deflection for All Specimens with No. 6 Bars.....	40
Figure 44. Load vs. Midspan Deflection for All Specimens with No. 6 Bars .....	40
Figure 45. Load vs. Reinforcement Strain (East) for All Specimens with No. 6 Bars .....	41
Figure 46. Load vs. Reinforcement Strain (West) for All Specimens with No. 6 Bars.....	42
Figure 47. Load vs. North Interface Displacement for All Specimens with No. 6 Bars .....	43
Figure 48. Load vs. South Interface Displacement for All Specimens with No. 6 Bars .....	43
Figure 49. Strain Variation Observed at the Top of the UHPC Pocket in U-6-8-I.....	44
Figure 50. Side View of the UHPC Pocket in Specimen U-6-5-I-E After Failure Showing Splitting Cracks .....	45
Figure 51. Side View of UHPC Pocket in Specimen U-6-6-I-E After Failure Showing the Effect of Prying Action.....	46
Figure 52. Top of the UHPC Pocket in Specimen U-6-7-I After Failure .....	46
Figure 53. Specimen U-6-8-I After Failure .....	47

Figure 54. Stress-Strain Relationship for Reinforcing Steel.....	49
Figure 55. Constitutive Model for UHPC and VHPC .....	50
Figure 56. Load vs. Strain at Bottom of Compression Reinforcement for Specimens with Two No. 4 Bars at Top and Bottom of Beam .....	51
Figure 57. Load vs. Strain at Bottom of Compression Reinforcement for Specimens with Two No. 4 Bars at Top and Two No. 7 Plus One No. 6 at Bottom of Beam.....	52
Figure 58. Load vs. Strain at Bottom of Compression Reinforcement for Specimens with Two No. 6 Bars at Top and Bottom of Beam .....	52
Figure 59. Load vs. Strain at Bottom of Compression Reinforcement for Specimens with Two No. 6 Bars at Top and Two No. 8 Plus One No. 7 at Bottom of Beam.....	53
Figure 60. Load vs. Strain at Bottom of Compression Reinforcement for Specimens with Two No. 4 Bars at Top and Two No. 8 at Bottom of Beam with VHPC .....	53
Figure 61. Method for Selecting Strain in Compression Bars at Ultimate .....	54
Figure 62. Strain Variation Observed at the Top of the UHPC Pocket in U-4-5-I-E .....	58
Figure 63. Strain Variation Observed at the Top of the UHPC Pocket in U-4-6-I-E.....	58
Figure 64. Strain Variation Observed at the Top of the UHPC Pocket in U-4-3-I.....	59
Figure 65. Strain Variation Observed at the Top of the UHPC Pocket in U-4-4-I.....	59
Figure 66. Strain Variation Observed at the Top of the UHPC Pocket in U-4-6-I-E.....	60
Figure 67. Strain Variation Observed at the Top of the UHPC Pocket in U-6-5-I-E.....	60
Figure 68. Strain Variation Observed at the Top of the UHPC Pocket in U-6-7-I.....	61

## List of Tables

Table 1. Test Matrix.....	4
Table 2. Concrete Properties of Precast Beams .....	12
Table 3. Reinforcing Bar Properties .....	13
Table 4. UHPC and VHPC Mixture Proportions.....	15
Table 5. Pocket Filler Material Properties .....	16
Table 6. Test Results for Specimens with No. 4 Bars .....	23
Table 7. Test Results for Specimens with No. 6 Bars and UHPC .....	38
Table 8. Average Strain Gauge Measurements in Specimens with No. 4 Bars.....	47
Table 9. Average Strain Gauge Measurements in Specimens with No. 6 Bars.....	48
Table 10. Equations for Steel Stress and Strain.....	49
Table 11. Parameters for UHPC Constitutive Model .....	50
Table 12. Maximum Strains and Stresses in Tension Reinforcement .....	55

# **1. INTRODUCTION**

## **1.1. Adjacent Precast Member Connections**

Bridges with adjacent precast members are suitable for short spans, places with low clearances and for accelerated bridge construction or replacement. This bridge system offers inherent advantages of economy, rapid construction and high torsional stiffness. However, the occurrence of reflective cracks in the deck persists to be the “Achilles heel” for this quick to implement and economical bridge system. The issue of reflective cracks in composite or non-composite toppings of bridges with adjacent precast box beam bridges has been prevalent since the very first details for the bridge system were devised and implemented. Through research, experimentation and experience the connection details have been updated to explore solutions to prevent or at least abate reflective cracking in bridges with adjacent precast members. The research presented in this report was initiated to develop a spliced connection between adjacent box and voided slab bridge beams, which would alleviate the problems of shear key failure and reflective cracking. This report is focused on the experimental and analytical work performed to establish the minimum splice length for uncoated No. 4 and No. 6 bars required to form a connection of sufficient strength and ductility.

The issues of shear key failure and associated reflective cracks in the bridge topping have been extensively detailed in the state-of-the-art report by Russell (2009). Traditionally, adjacent precast member bridge beam connections have made use of a grouted shear key detail, partial or full beam depth and transverse post-tensioning (PT) to attempt to produce a monolithic behavior in the bridge superstructure. It has been observed in the US that the traditional detail has been susceptible to failure. Moreover, the transverse PT has proven to be insufficient in producing a uniform monolithic behavior in the superstructure. Transverse PT is most effective at the discrete locations of application. The compressive effect of transverse PT is reduced progressively at locations further from point of application. As shear key failure is initiated in the joints of the adjacent precast member bridge system, the load distribution between adjacent beams is adversely affected. Essentially, the traditional grouted connection has proven to be insufficient in resisting the shears and especially the moments generated on the connection by traffic loads, intrinsic loads such as shrinkage and environmental effects such as temperature gradients.

## **1.2. Ultra-High Performance Concrete Connections**

Recently, Ultra-High Performance Concrete (UHPC) has been used in connections between full depth precast deck panels (Graybeal 2010), between flanges of decked bulb-tee beams (Perry and Royce 2010), and between full depth deck panels and supporting beams (Graybeal 2012). There is not yet a universally accepted definition of UHPC, but Russell and Graybeal (2013) define it as a cementitious-based composite material with discontinuous fiber reinforcement, compressive strengths above 21.7 ksi, pre-and post-cracking tensile strengths above 0.72 ksi, and enhanced durability via their discontinuous pore structure. Due to the high compressive and tensile strength of UHPC, non-prestressed steel reinforcing bars can be developed in much shorter lengths than in conventional concrete (Graybeal 2010). This allows connections between precast elements, which have reinforcement extending into the connection,

to be much smaller with UHPC than with typical concrete. Therefore, UHPC was investigated as a filler material for the connections developed in this research.

A popular proprietary UHPC is Ductal, produced and distributed by LaFarge. It is one of the materials used in this project. One drawback to Ductal, and other proprietary UHPC formulations, is its high cost. An alternative concrete mixture was developed in a previous research project, and it was also investigated in this project as a filler material for the connections. The properties of this material do not meet the suggested minimums to be defined as UHPC, so, for the purposes of this report, it is referred to as Very High Performance Concrete (VHPC). The compressive and tensile strengths are not as high as UHPC, but being non-proprietary, and containing small coarse aggregate, it is much less expensive.

### 1.3. Connection Testing Program

In this research an alternative means to achieve connections between adjacent beams was sought. The main focus of this research was to incorporate a structural connection between adjacent members that can resist the aforementioned load effects. To that means, a spliced connection between adjacent members was proposed (see Figure 1). This report outlines the preliminary testing program which was focused on establishing the minimum length of splice required to provide sufficient strength and ductility to the connection using UHPC or VHPC as the connection filler material. The results of the experimental program and the analysis performed to verify the results are presented.

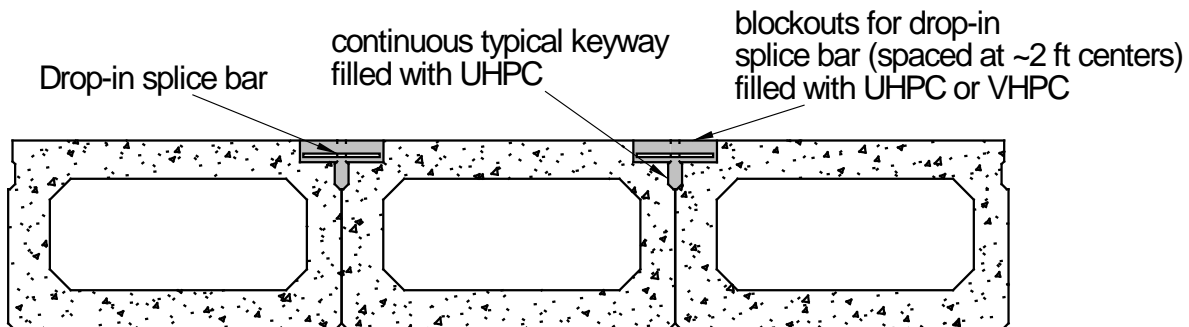


Figure 1. Adjacent Box Beam Connection with Drop-In Splice Bar

## 2. PURPOSE AND SCOPE

The purpose of this research was to determine the minimum splice length for uncoated No. 4 bars and No. 6 bars in UHPC and VHPC concrete. A total of 15 beams, 12 in tall by 10 in wide by 8.5 ft long, were precast with conventional concrete, and included a block-out pocket to accommodate a splice. The tension bars were spliced in the pocket, which was then filled with either VHPC or UHPC. The beams were tested to place the splice location in a region of constant moment, and were loaded monotonically to failure.

Strain gauges could not be placed on the tension reinforcement, because the waterproofing disrupts the bond between the steel and concrete. Instead, the compression reinforcement was instrumented, and a strain compatibility analysis was performed to determine the stress and strain in the tension reinforcement at failure. Splice lengths were varied to determine the shortest length which resulted in the bar exceeding its yield strength, and exceeding a strain at ultimate of 0.005.

### **3. METHODS**

#### **3.1. Specimen Details**

The specimens were 8.5 ft long simply supported reinforced concrete beams with a block-out pocket at midspan. The tension reinforcing bars were not continuous at the midspan, and a bar was placed across the discontinuity to form the splice connection. The cross-sectional size of the pocket was kept consistent between specimens. The length of the pocket was varied according to the splice length under consideration. The main tension reinforcement was either two No. 4 bars or No. 6 bars depending on the specimen. These bar sizes were considered for forming the connections between adjacent beams in bridges based on results of experimental testing reported by Perry and Weiss (2009). In the first four specimens tested, the area of steel in compression was the same as that in tension. This was, however, revised in later tests after observing the test results from initial specimens and is discussed in greater detail in the analysis of results. The typical details of the test specimens are summarized in Table 1. The typical details of the initial test specimens with UHPC are shown in Figure 2 and the typical details of the modified (greater area of compression reinforcement) test specimens with UHPC are shown in Figure 3. Figure 4 presents the details of the specimens with VHPC.

Critical information needed from the testing was the stress and strain in the spliced reinforcing bars. To determine if a splice length is adequate to develop the yield strength of the bar, the stress in the bar must be known. Unfortunately, this measurement cannot be made directly with a bonded electrical resistance strain gage on the tension steel, because the water proofing required to protect the gage from the concrete destroys the bond between the bar and the concrete. Therefore, another method was needed to determine the forces in the spliced bars during the tests.

**Table 1. Test Matrix**

Specimen Designation	Tension Steel	Splice Length, in	Pocket Length, in	Pocket Filler	Compression Steel	Concrete Strength, ksi
U-4-5-I-E	2 No. 4s	5	11	UHPC	2 No. 4s	8
U-4-6-I-E		6	13			
U-4-3-I		3	7		2 No. 7s and 1 No. 6	5
U-4-4-I		4	9			
U-4-5-II		5	11			
V-4-5-I		VHPC	5	11	2 No. 8s	5
V-4-6-I			6	13	2 No. 8s	5
V-4-5-II			5	15	2 No. 8s	5
V-4-3-I			3	17	2 No. 8s	5
V-4-4-I			4	21	2 No. 8s	5
V-4-4-II			4	9	2 No. 8s	5
U-6-5-I-E			2 No. 6s	5	11	UHPC
U-6-6-I-E	6	13				
U-6-7-I	7	15		2 No. 8s and 1 No. 7	5	
U-6-8-I	8	17				

The specimen nomenclature is as follows,

U/V-BR-SL-No-DS

Where,

U/V = Material used in pocket. U = UHPC, V = VHPC

BR = Tension reinforcing bar size, in

SL = Length of splice, in

No = Serial number for each specimen type on the basis of splice lengths

DS = Specimen design. E = equal area of steel in tension and compression

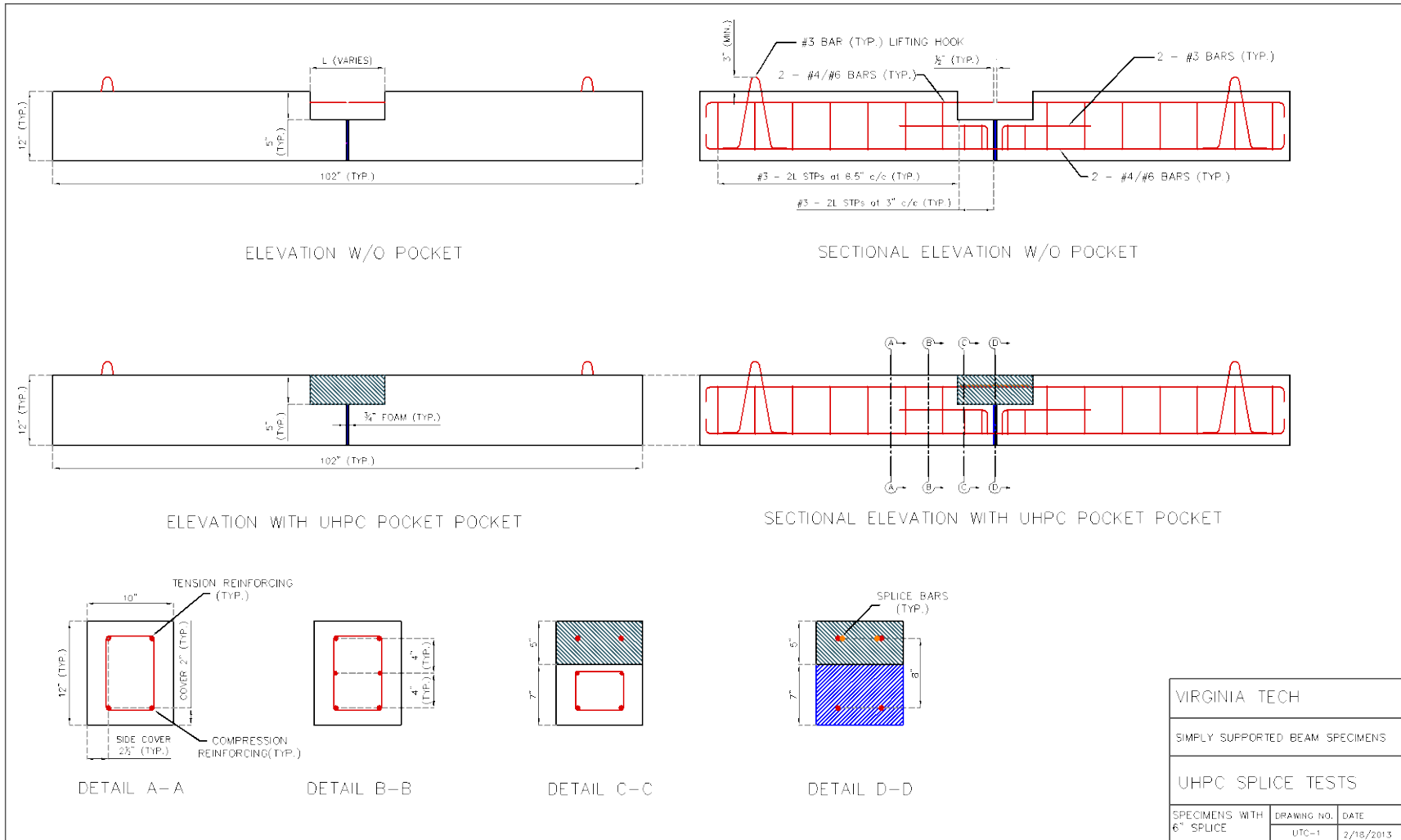
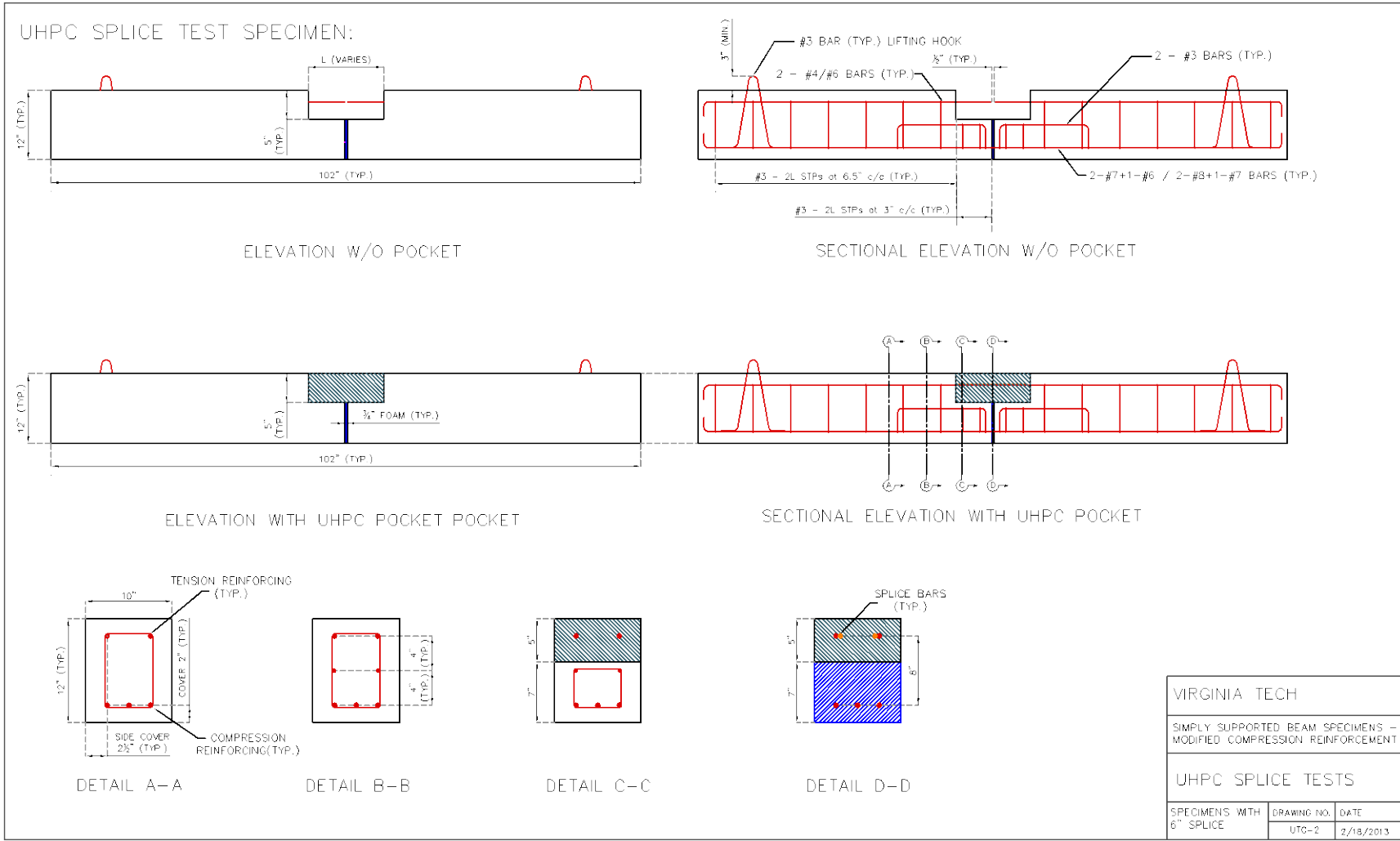


Figure 2. Typical Details of Initial Test Specimens



**Figure 3. Typical Details of Modified Test Specimens**

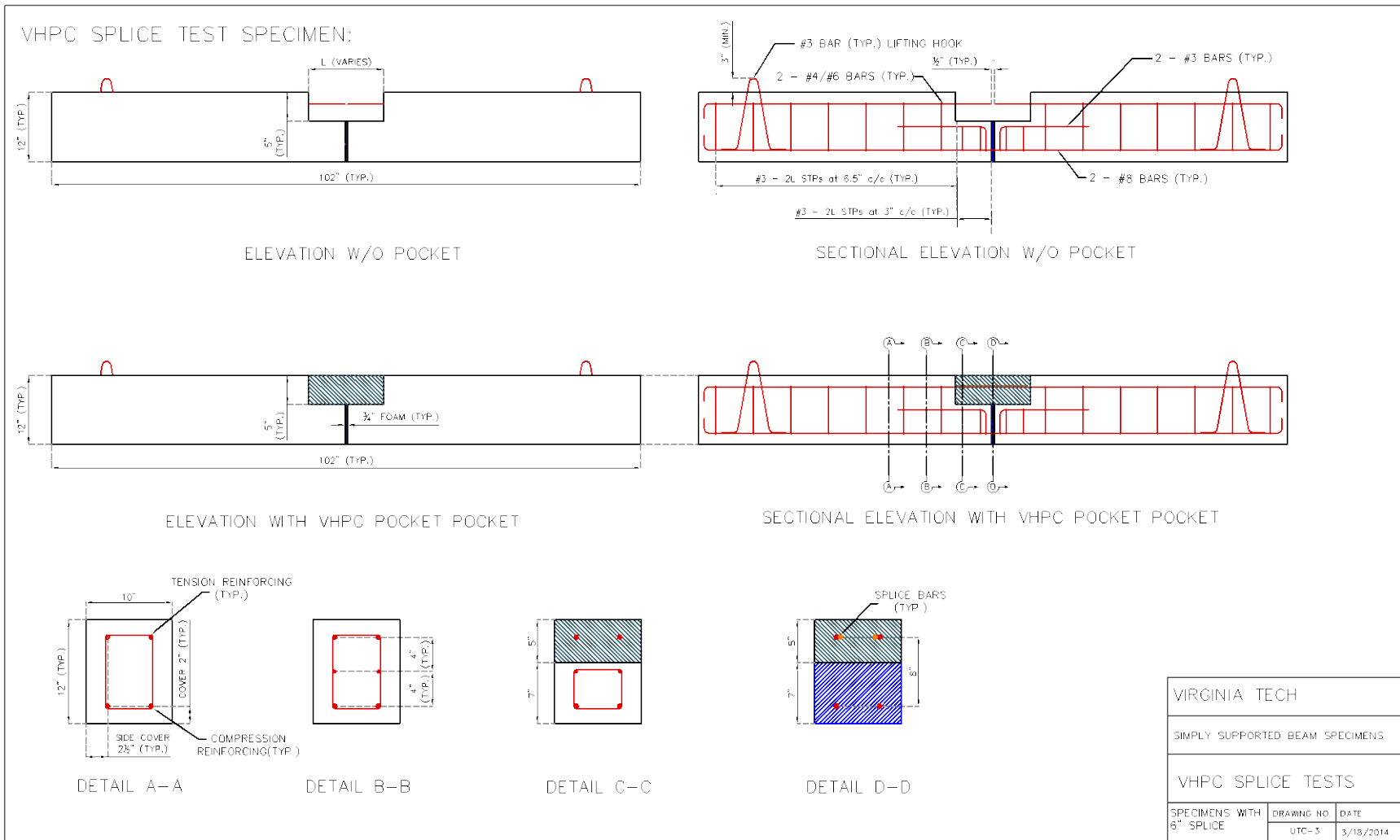
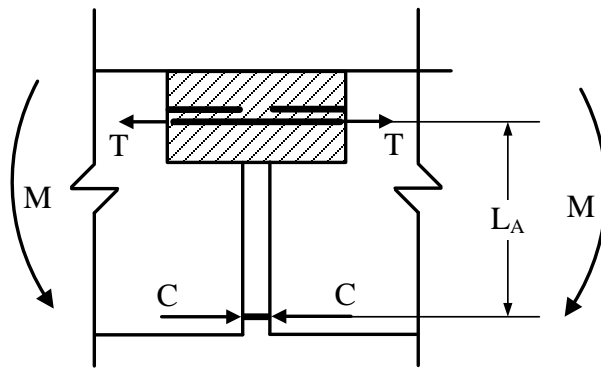


Figure 4. Typical Details of VHPC Test Specimens

At the midspan of the beam, beneath the splice pocket, a  $\frac{3}{4}$  in. thick foam pad was placed vertically to separate the left and right sides of the precast element. In this way, the bottom layer of reinforcement alone carried the compression at this location. This was expected to simplify the calculation of the stress in the tension reinforcement, by eliminating the uncertainty in determining the moment arm between the tension and compression forces in the beam. In this way, there was no need to assume a stress block and a location of the centroid of the compression block. Also, since the total tension must equal the total compression, after the pocket filler material had cracks with widths too wide to allow the fibers to carry tension, all tension must be in the reinforcing steel alone. The compression bars were strain gaged to allow the calculation of the compressive force. The gap in the concrete facilitated the calculation of tensile force which would indicate whether the reinforcing steel in tension yielded prior to the failure of the specimen. The mechanics of the specimen section at the area of interest are shown in Figure 5.



**Figure 5. Beam Mechanics: Tension Equals Compression for Equilibrium**

The section of the precast element under the UHPC or VHPC pocket was reinforced with longitudinal No. 3 bars and stirrups as shown in Figure 2, Figure 3, and Figure 4. These were included to ensure that no premature failure would occur in the precast section of the specimen.

### 3.2. Test Setup

The test setup is shown in Figure 6. The test configuration placed the splice in the region of maximum constant bending moment. The specimens were tested in an inverted configuration so that the cracking patterns in the UHPC/VHPC pocket could easily be observed. The load applied through the actuator was measured by a single load cell (maximum capacity 50 kips). Vertical deflections were measured by three wire potentiometers connected to the beam ends and midspan of the beam. The interface between UHPC/VHPC and beam concrete was instrumented with LVDTs (on the east face) to observe the occurrence of cracks at the concrete – UHPC/VHPC interface. The reinforcement in the compression zone was instrumented with strain gauges. In the specimens which had two compression bars, both reinforcing bars were instrumented. In the specimens which had three compression bars, the two outermost reinforcing bars (see Figure 2) were instrumented. Additionally, locating discs for a DEMEC (Demountable MEchanical) extensometer were attached to the top of the UHPC pocket and the west face of all

specimens to measure surface deformations at different depths at midspan (top fiber, tensile reinforcement depth, mid-depth of beam and compressive reinforcement depth).

### 3.3. Test Procedure

The testing program consisted of loading each beam statically to failure in a four point loading setup. The spacing of the bolt patterns on the floor beams did not allow for a uniform distance between supports and loading points. Hence, the spacing between the supports was increased to 3 ft. The corresponding reduction in distance between the support and loading point caused the span to be at the threshold of the deep beam definition per ACI 318. ACI defines a deep beam as one having a ratio of the clear span between a support and the nearest loading point to the depth of the beam less than 2.0. The ratio in the test beam was 2.5.

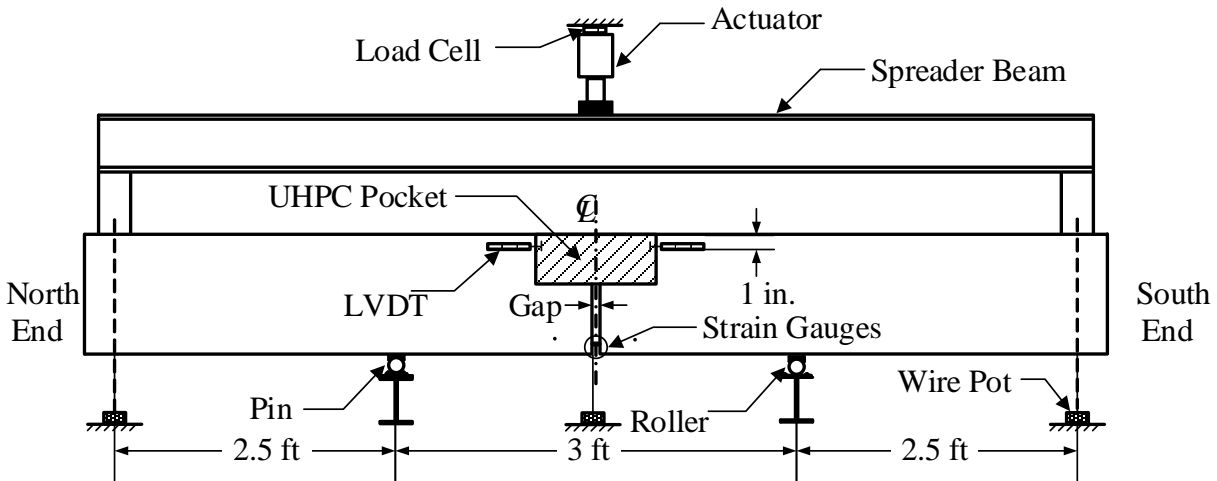


Figure 6. Test Setup

The loading on the beams was applied monotonically at pre-determined increments with pauses to mark cracks and make DEMEC measurements. Load increments of 1000 to 2000 lb were applied to specimens with No. 4 bars until the first crack in the UHPC/VHPC pocket was observed. The load application was then increased to 2500 to 3000 lb. Similarly, load increments of 2000 to 3000 lb were applied to specimens with No. 6 bars followed by increments of 5000 to 6000 lb after first UHPC crack was observed. The actual rate of loading during load application was difficult to control due to the nature of the manually operated electric hydraulic pump. Hence, the load application was accomplished in small steps. To ensure correct load application the responses from wire potentiometers, strain gauges on compression reinforcement and the DEMECs were monitored for the first three load application steps. If the corresponding increase in deflections at the ends and/or the increases in strains were found to be unequal then the beam was unloaded and the actuator was repositioned to ensure equal load application at both ends of the specimen and across the cross-section of the specimen.

The System 5000 data acquisition system (DAQ) was used to record data. The DAQ was programmed to read and record data at 10 Hz. Although the test itself was static it was important to record response of the specimen to instantly changing conditions such as the occurrence of cracks or tension reinforcement slip. The data recording was started after the specimen was positioned on the supports prior to the placement of the spreader beam. Hence, the test data does not directly include the effect of self-weight of the specimen on the test results. Similarly, the baseline reading for DEMEC readings was made after the beam was positioned on the supports. The effect of self-weight was found to be small in comparison to applied loads on the results of the splice tests.

### **3.4. Material Properties**

Tests were performed to determine the material properties of the reinforcing steel, conventional concrete, UHPC and VHPC used in the tests. One of the advantages of adjacent precast member bridges is that they can be rapidly constructed. Therefore, all tests were done at the relatively early age for the filler material of 7 days. Concrete material tests were performed immediately prior to the initiation of each splice test.

For the conventional concrete, compressive strength, splitting tensile strength and modulus of elasticity tests were performed. Three 4 in by 8 in cylinders were tested for each property at the time of initiation of the test.

For the UHPC and VHPC, compressive strength, splitting tensile strength and modulus of elasticity tests were performed. Three 4 in by 8 in cylinders were tested for each property at the time of initiation of each test. In addition, 4 in by 4 in by 14 in flexural beam tests were conducted per ASTM C1018, and direct tension mortar briquette (dog bone) tests were performed per a modified version of ASTM C190. These tests were performed to investigate and compare the post-cracking tensile strength of the VHPC and UHPC used in the splice block-out pockets.

Figure 7 shows the set up for the modified dog bone test. The test was performed in a 34,000 lb capacity screw-driven universal test machine. The test was performed under displacement control, so the post-cracking behavior could be observed. The load and cross-head displacement were recorded, and high resolution photographs were taken to determine crack widths at known loads after initial cracking.



**Figure 7. Dog Bone Test Setup**

## **4. RESULTS**

This section presents test observations and measurements. First the material property testing results are presented. Then the results of the splice tests are presented separately for specimens with No. 4 bars and specimens with No. 6 bars. Refer to Table 1 for specimen designation.

### **4.1. Material Properties**

#### *4.1.1. Concrete Properties*

The precast beams were cast on three occasions. For each placement, specimens were made to determine compressive strength, splitting tensile strength and modulus of elasticity. The precast pieces were moist cured for seven days prior to removal from the forms. After stripping the forms, the beams were stored in the lab until placement of the splice filler and subsequent testing. The properties of the concrete are presented in Table 2. For the specimens with VHPC, splitting tensile strength and modulus were only tested at the end of the testing program.

**Table 2. Concrete Properties of Precast Beams**

<b>Specimen Designation</b>	<b>Compressive Strength, psi</b>	<b>Splitting Tensile Strength, psi</b>	<b>Modulus of Elasticity, ksi</b>
U-4-5-I-E	7360	816	4090
U-4-6-I-E	7360	816	4090
U-4-3-I	7360	816	4090
U-4-4-I	3900	-	3590
U-4-5-II	3900	-	3590
V-4-5-I	4700	-	-
V-4-6-I	4700	-	-
V-4-5-II	4640	-	-
V-4-3-I	4890	-	-
V-4-4-I	4890	-	-
V-4-4-II	4640	-	-
End of Test VHPC	4720	351	3400
U-6-5-I-E	7360	816	4090
U-6-6-I-E	7360	816	4090
U-6-7-I	3900	-	3590
U-6-8-I	3900	-	3590

#### 4.1.2. Reinforcing Properties

The bars used for the splices and as the compression reinforcing were tested to determine the stress-strain behavior. Samples of each bar size were placed in the Satec Universal test machine, and gripped at each end with hydraulically operated grips. For initial samples, strains were measured only with a clip-on 2 in gauge length extensometer. Strains were measured on later samples using both the clip-on extensometer, and bonded electrical resistance strain gauges. The clip on extensometer was removed at a strain of 0.03 so that it would not be damaged. After removal of the gage, the cross-head displacement, and the measured distance between the cross-heads was used to calculate the strains.

Figures 8, 9, 10, and 11 present the stress-strain plots for the No. 4, No. 6, No. 7 and No. 8 bars, respectively. It is to be noted that the strains for the No. 8 bars in Figure 11 are calculated from the full length of the bar. The diameter of the No. 8 bars was too large for the extensometer to grip the bar specimens. Therefore, the strains for No. 8 bars were calculated from the full 24 in gauge length of the bar Table 3 presents the key properties of the reinforcement. Note that bars designated U-bars were used in the UHPC pockets and those designated V-bars were used in the VHPC pockets.

**Table 3. Reinforcing Bar Properties**

Bar Size	Filler Material	Modulus of Elasticity, ksi	Yield stress, ksi	Strain at onset of strain hardening	Ultimate Strength, ksi	Ultimate Strain
No. 4	UHPC	29,000	62.0	0.0077	102	0.140
No. 6	UHPC	29,000	60.0	0.0077	102	0.164
No. 7	UHPC	29,000	62.0	0.0072	102	0.136
No. 8	UHPC	29,000	69.5	0.0055	104	0.176
No. 4	VHPC	29,000	69.0	0.0062	109	0.106
No. 8	VHPC	29,000	69.5	0.0055	104	0.176

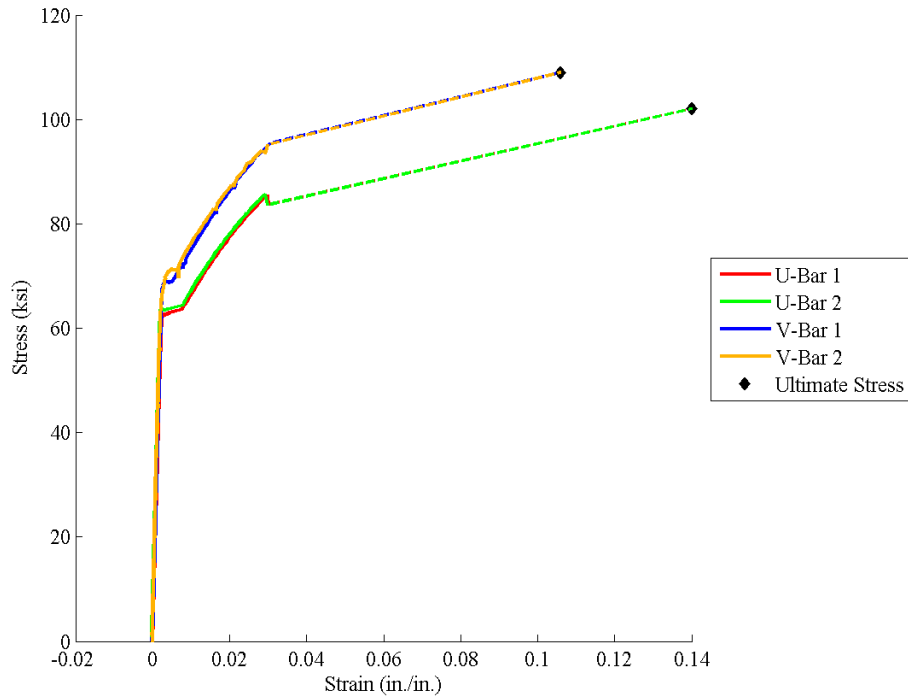


**Figure 8. Stress vs. Strain Plot for No. 4 Bars**

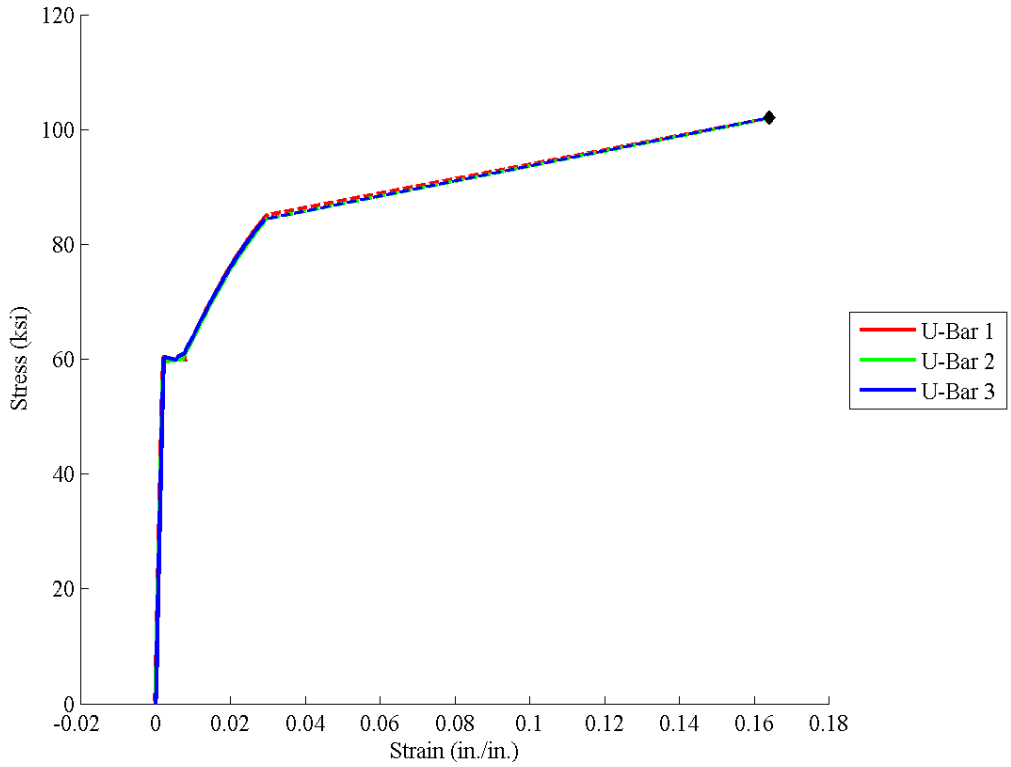


**Figure 9. Stress vs. Strain Plot for No. 6 Bars**

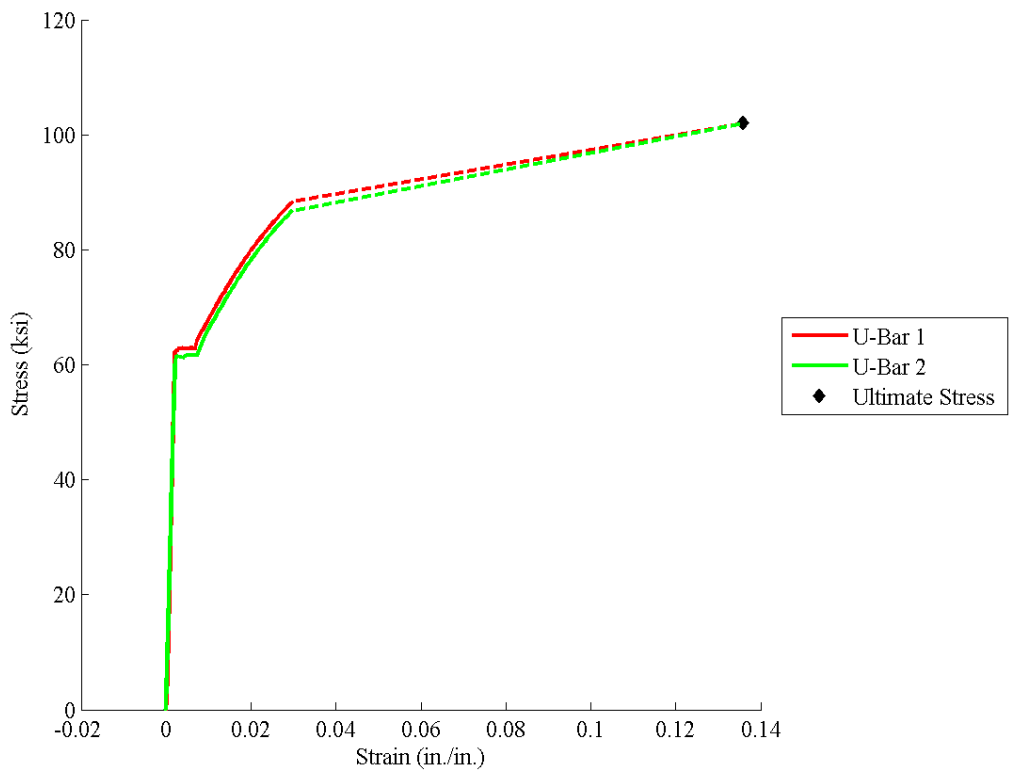


**Figure 10. Stress vs. Strain Plot for No. 7 Bars**

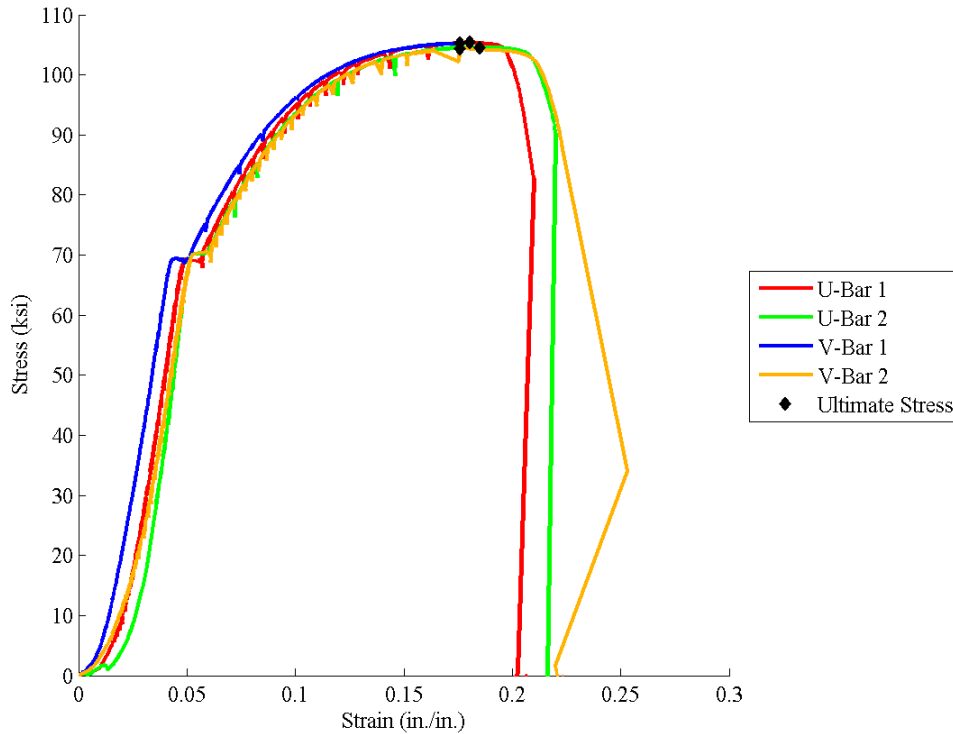


**Figure 11. Stress vs. Strain Plot for No. 8 Bars**

#### 4.1.3. Splice Pocket Filler Properties

The splice pockets were filled with either a proprietary UHPC (Ductal by LaFarge) or a very high performance concrete (VHPC), with a mix design developed by the researchers. Table 4 presents the mix designs for the two filler materials. LaFarge delivers Ductal in premix bags, and does not provide the mix design. The proportions presented in Table 4 are from Graybeal (2006) and represent a typical formulation for Ductal. The VHPC mix design was developed using proportions presented in Akhnoukh (2008) as a starting point, but adding 1 in. long steel fibers at 2% by volume to provide tensile strength.

**Table 4. UHPC and VHPC Mixture Proportions**

Constituent	UHPC, lb/cu. Ft	VHPC, lb/cu. Ft
Cement	44.44	41.50
Silica Fume	14.44	8.90
Fly Ash	NA	8.90
Ground Quartz	13.15	NA
Fine Sand	63.7	53.70
¼ in. max course aggregate	NA	23.00
water	6.82	11.80
superplasticizer	1.92	0.75 – 1.05
Steel fibers	9.74	9.80
Water/cementitious	0.12	0.20
total	44.44	41.50

The splice pockets were filled two at a time, and tested seven days after placement. Samples were made from each batch to determine compressive strength, splitting tensile strength, and modulus of elasticity. In addition, from one batch of the VHPC, 4 in by 4 in by 14 in modulus of rupture bars were made to investigate the post-cracking ductility of the material. Also, mortar briquettes were made from earlier batches of UHPC and VHPC to investigate direct tensile strength, and post-cracking toughness. A key parameter of interest is the crack width at which the fibers can no longer carry tension across the open crack. Table 5 presents the material properties of each batch of UHPC and VHPC.

**Table 5. Pocket Filler Material Properties**

Placement	Specimens	Age at Testing, days	Compressive Strength, ksi	Splitting Tensile Strength, ksi	Modulus of Elasticity, ksi
10/19/12	UHPC	7	14,000	3680	6840
11/6/12	UHPC	7	13,200	3070	6460
11/22/12	UHPC	14	23,800	N/A	8530
12/13/12	UHPC	8	13,500	3140	6670
6/6/13	UHPC	7	20,200	2200	8080
6/19/13	UHPC	8	20,700	2100	8150
6/19/13	UHPC	9	20,500	2390	8280
6/4/13	UHPC	7	19,300	2670	8210
6/6/13	UHPC	9	20,700	2390	8090
1/13/14	VHPC	8	12,400	1660	5440
1/13/14	VHPC	9	13,500	N/A	5680
2/3/14	VHPC	7	12,900	1620	5750
2/11/14	VHPC	10	13,800	1750	5250

Figure 12 presents the results of the modulus of rupture bar tests made from the concrete cast on 2/13/14 and performed when the VHPC was seven days old. The average compressive strength of the VHPC at seven days was 12,900 psi. The test was performed in accordance with ASTM C-1018, which requires the measurement of the midspan displacement to determine the post-cracking toughness of fiber reinforced concrete. The figure illustrates how the VHPC can continue to carry load after the first crack, which occurred on all three test specimens at around 1500 psi tension at the bottom of the beam. After first crack, the beams continued to support increasing loads out to a midspan displacement of about 0.04 in. After that, the beam continued to deform, but the load carried decreased until the midspan displacement had reached between 0.09 and 0.105 in.

The average peak equivalent bending stress was 2270 psi. This is not a true stress, because it is calculated as:

$$f_t = \frac{My}{I} = \frac{\frac{P}{2} \cdot 4in \cdot 2in}{\frac{1}{12}(4in)^4} = \frac{P}{5.333in^2} \quad (1)$$

With:

- $f_t$  = stress at extreme fiber of flexural beam, psi
- $M$  = moment in constant moment region of flexural beam, in-lb

- $I =$  moment of inertia of beam, in<sup>4</sup>
- $y =$  distance from centroid of cross-section to extreme fiber, in
- $P =$  applied load, lb

This equation assumes an uncracked section, so it is invalid after the first crack. However, the stress calculated with this formula after cracking can still be used to compare the behavior of different types of fiber reinforced concrete, when the fibers carry significant tension after cracking.

For comparison, Figure 13 presents results of a flexural beam test of UHPC (Ductal by LaFarge). These tests were performed on UHPC that was also 7 days old, had not been steam or heat treated, and had an average compressive strength at time of testing of 15,000 psi. The average cracking stress of these specimens was 1500 psi, which was the peak bending stress. The post-cracking plateau was at an equivalent bending stress of 1300 psi. This behavior is very similar to the VHPC tested at seven days in this research program. Note that the vertical axis in Figure 13 is the force applied to the beam in lbs. To convert to the equivalent stress, divide by 5.333 in<sup>2</sup> (see Equation 1).

Figure 14 presents the load vs. cross-head displacement for the dog bone tests for VHPC and Figure 15 presents similar tests on UHPC. Note that these tests were performed when the specimens were over one year in age. However, neither type of concrete had been steam nor heat treated. As can be seen by comparing the results of the dog bone tests, both materials can carry direct tension stress after the first crack has opened on the specimen. The UHPC has a more gradual loss of tension on the descending branch of the curve, but the VHPC is also able to carry tension through continued crosshead displacement.

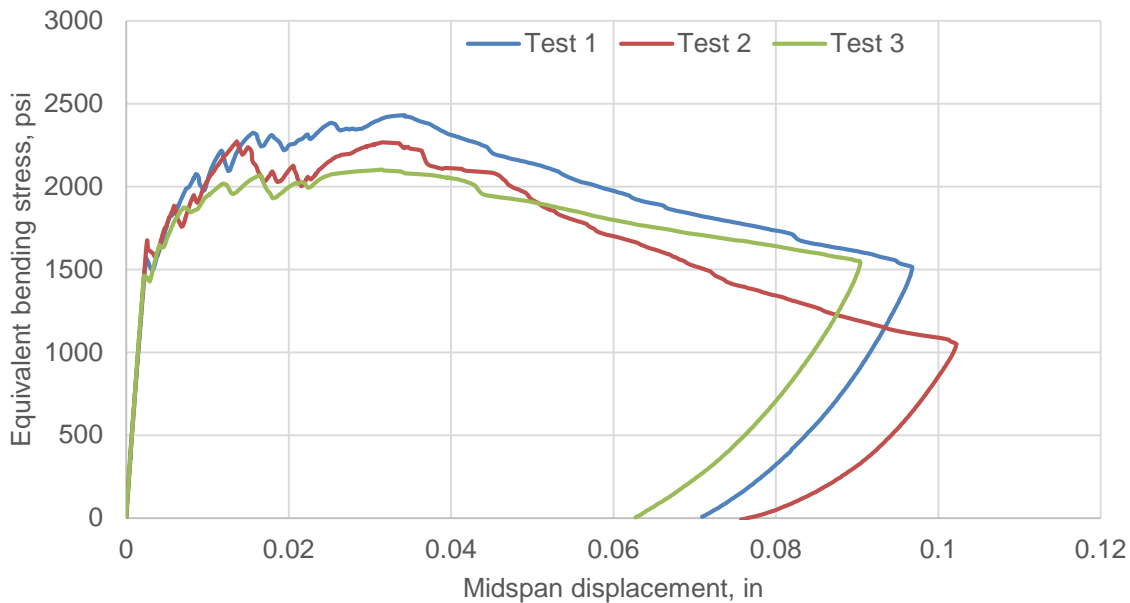


**Figure 12. Flexural Beam Test Results for VHPC at 7 Days**

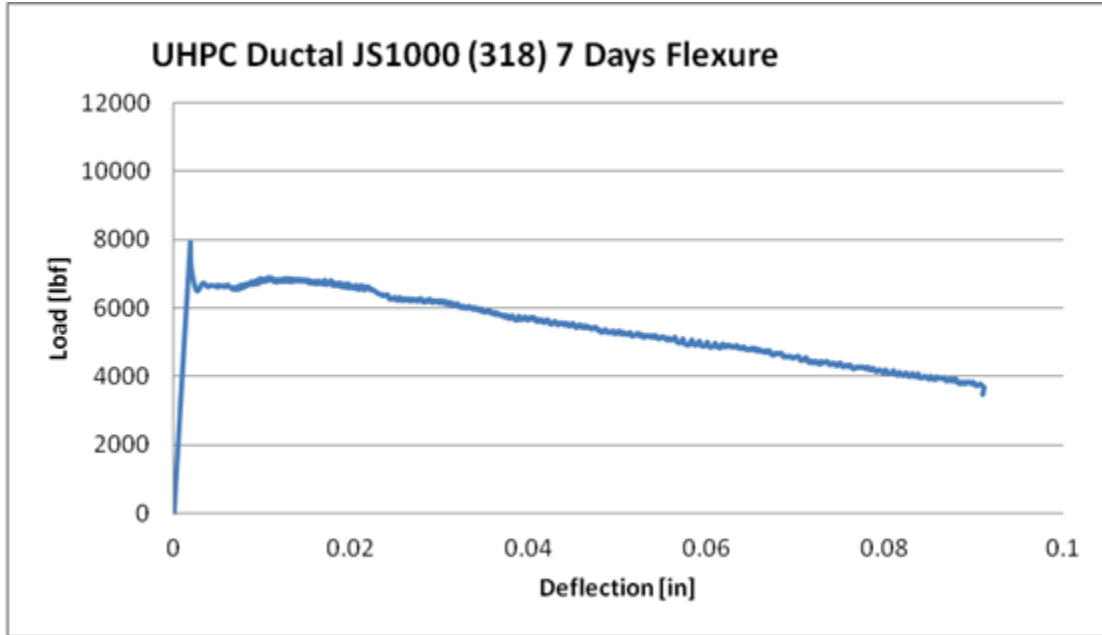


Figure 13. Typical 7 Day Flexural Beam Test Results for Untreated UHPC

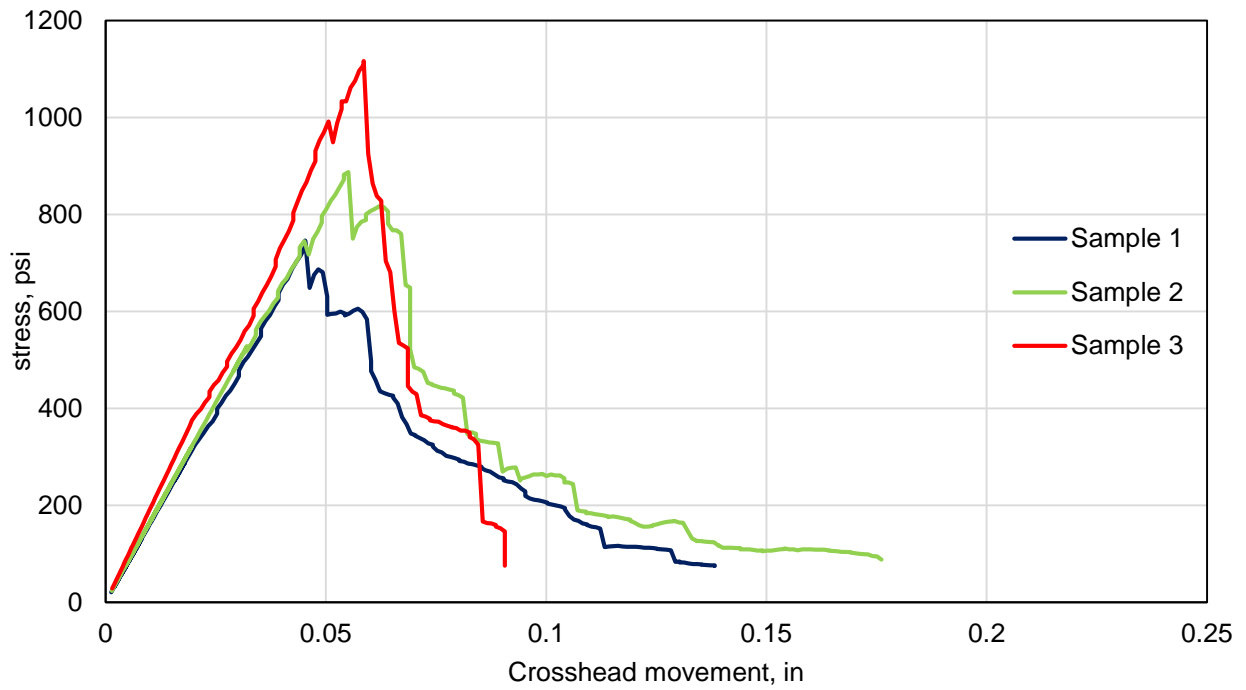
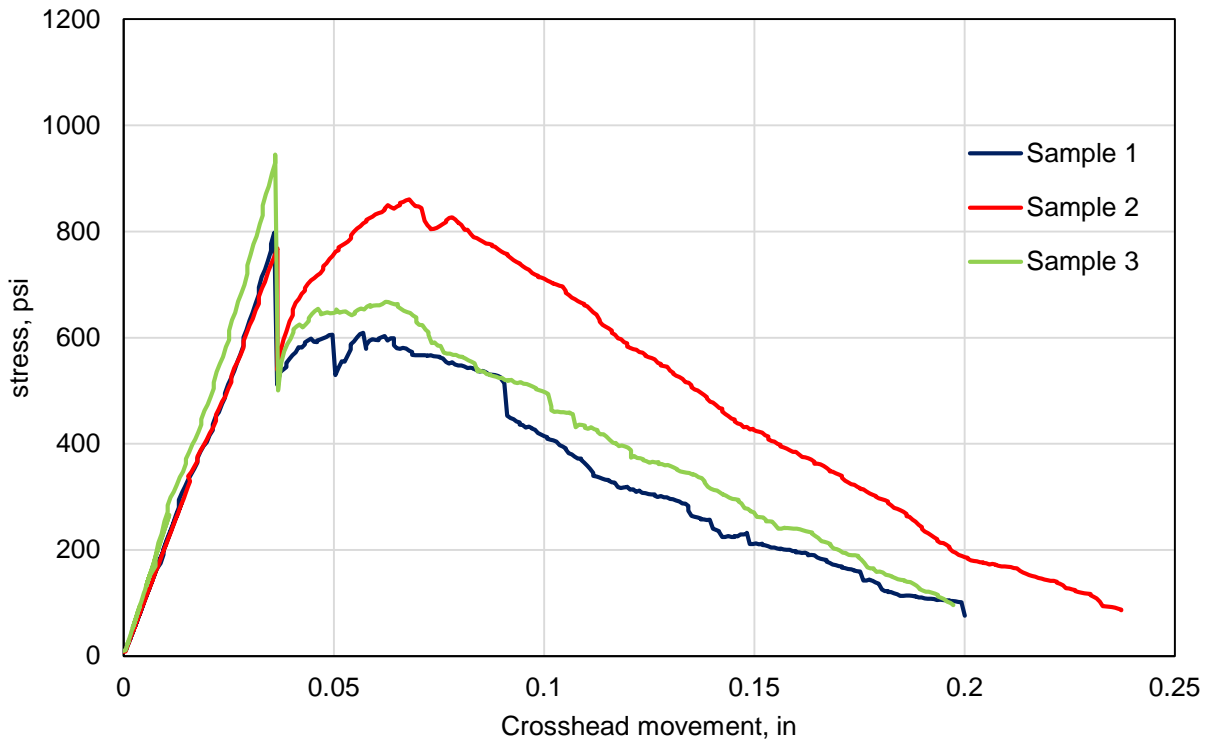
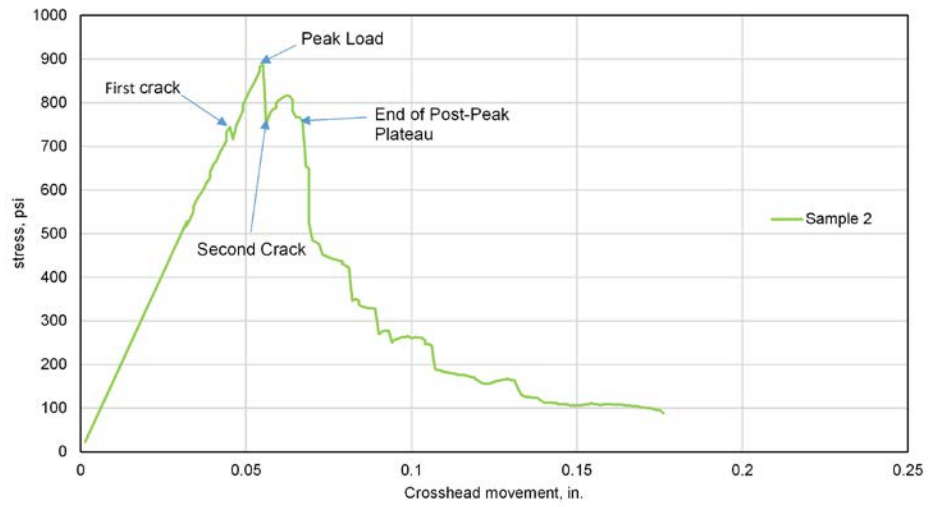
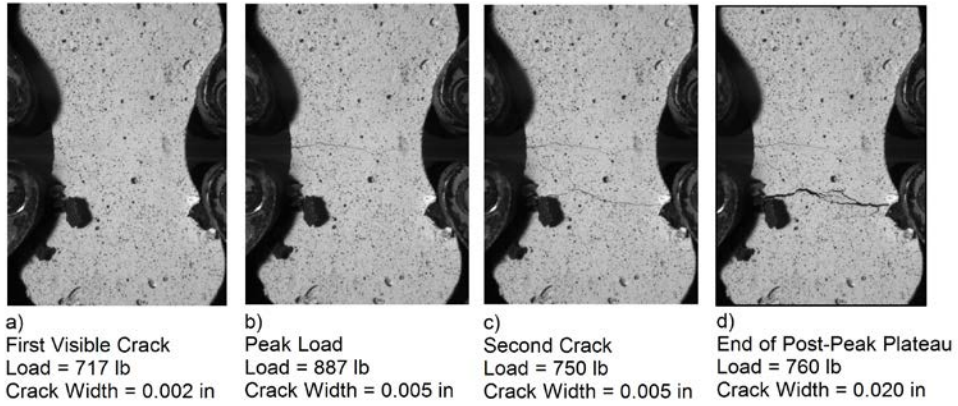


Figure 14. UHPC Dog Bone Test



**Figure 15. UHPC Dog Bone Test**

For one specimen of each type of concrete, a series of high resolution photographs was taken during testing. Figures 16 and 17 present key points during testing. For the VHPC the points presented are the first visible crack, the peak load, immediately following the peak load when a second crack appeared and the stress dropped rapidly, and the end of the post-peak plateau. For the UHPC specimen, at the time the specimen reached its peak load, there was no visible cracking. However, since the camera only captured images of one side of the dog bone, the cracking could have been on the opposite side of the specimen. The first crack became visible after the second peak, just as the load began to drop off.



**Figure 16. Cracking Behavior of VHPC Dog Bone Sample 2**

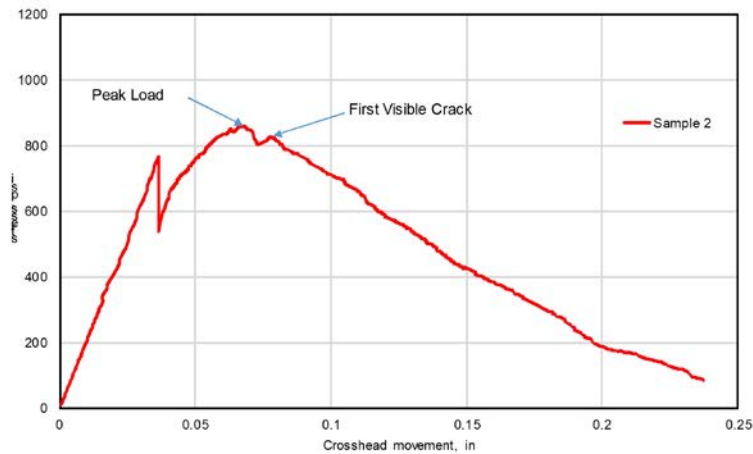
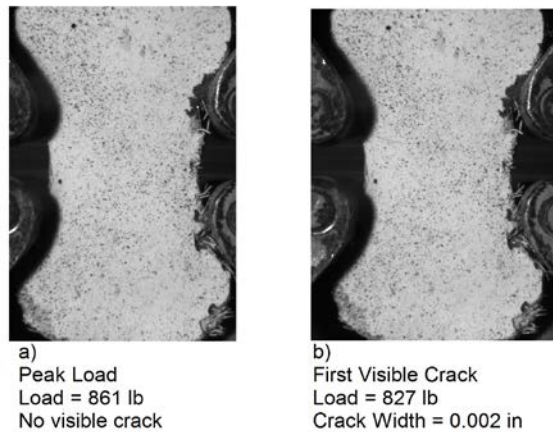


**Figure 17. UHPC Cracking Behavior**

It can be seen that the behavior of the UHPC and VHPC was similar prior to the peak load, but that the UHPC had a better post-peak behavior, sustaining higher loads at similar crack widths. Figure 18 is a comparison of the UHPC and VHPC specimens at a similar crack width on the descending branch. In both photographs, the crack width is 0.05 in. The UHPC, however, carried a higher stress across the crack (563 psi) than the VHPC (251 psi).

Although the post-peak behavior of the VHPC is not as good as the UHPC, the splice tests were performed to determine if the post-peak behavior of the VHPC is good enough to result in relatively short splice lengths within the material. Also note that while the VHPC performance is not as high as the UHPC, because it is non-proprietary, it is a lower cost material.

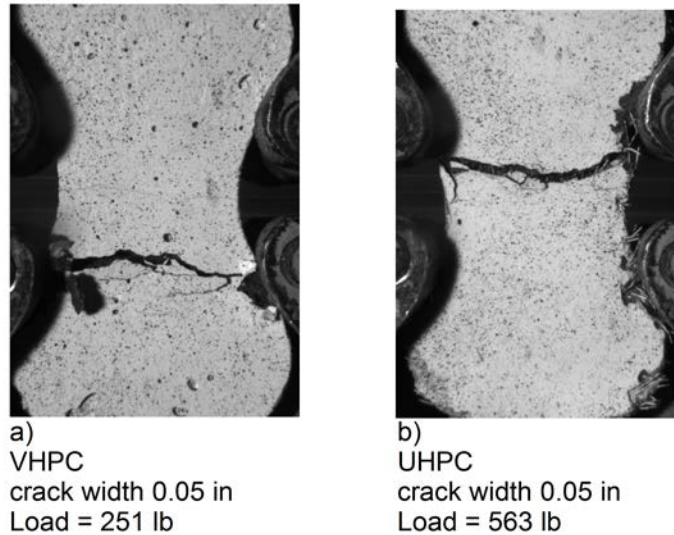


**Figure 18. Comparison of VHPC and UHPC Dog Bone Specimens with 0.05 in Cracks**

## **4.2. Splice Test Results for No. 4 Bars and UHPC and VHPC Splice Pocket Filler**

### *4.2.1. Summary of Test Results*

The splice lengths tested with No. 4 bars range from 3 in to 6 in. As discussed earlier the UHPC tests were performed in two stages. Specimens U-4-5-I-E and U-4-6-I-E were the first beams tested. The reinforcement details of these beams are shown in Figure 2 and, to reiterate, both the tension and compression reinforcement was two No. 4 bars. The remaining specimens were tested in the second phase of testing. The second stage UHPC beams, shown in Figure 3, contained two No. 4 bars as tension reinforcement and a combination of two No. 7 bars and one No. 6 bar as compression reinforcement. After observing the results from the UHPC tests, the VHPC specimens were designed with two No. 4 bars as tension reinforcement and two No. 8 bars as compression reinforcement (see Figure 4). Table 6 presents the cracking load, maximum load, and failure mode measured for each specimen.

Since there was no direct measurement of bar slip, a slipping failure deemed to be was characterized by a significant widening of a crack, or the pocket-to-precast interface opening, with a decreasing load. If there were no slip, increased crack width would be associated with increasing bar strain, bar stress, and therefore, applied load. The crack or interface opening wider with a decreasing load indicated that the bar must be slipping or debonding in the vicinity of the crack. The slipping was accompanied by splitting cracks in some of the specimens, and these are noted in Table 6 as slip/split failures. One specimen failed by rupture of the bar. Also note that the first two tests, U-4-5-I-E and U-4-6-I-E, which had equal amount of tension and compression reinforcement, had very ductile failures, since both top and bottom bars had yielded, and were strain hardening significantly. For both specimens, with large applied displacement, the load was not increasing significantly, so the tests were halted before any obvious slipping or splitting occurred.

**Table 6. Test Results for Specimens with No. 4 Bars**

Specimen Designation	Splice Length, in	Compression Reinforcement	First Cracking Load, lbs	Maximum Load, lbs	Failure Mode
U-4-5-I-E	5	2 No. 4s	7200	28,000	-
U-4-6-I-E	6	2 No. 4s	6900	26,500	-
U-4-3-I	3	2 No.7s and 1 No. 6	5800	15,700	slip
U-4-4-I	4	2 No.7s and 1 No. 6	7500	24,500	slip/split
U-4-5-II	5	2 No.7s and 1 No. 6	9000	29,600	slip/split
V-4-5-I	5	2 No. 8s	3,200	24,500	slip/split
V-4-6-I	6	2 No. 8s	3,000	28,700	slip/split
V-4-5-II	5	2 No. 8s	1,500	28,300	rupture
V-4-3-I	3	2 No. 8s	1,000	21,300	slip/split
V-4-4-I	4	2 No. 8s	2,000	21,800	slip
V-4-4-II	4	2 No. 8s	1,500	23,800	slip/split

The nominal strength of the specimens was calculated based on the nominal yield strength of the tension reinforcement and the moment arm between the compression and tension reinforcement. For this basic calculation, the contribution of the UHPC/VHPC to flexural strength is ignored.

$$A_s = 0.2 \text{ in}^2 \times 2 = 0.4 \text{ in}^2 \quad (2)$$

$$M_n = A_s f_y \times \text{moment arm} = 0.4 \text{ in}^2 \times 60 \text{ ksi} \times 8 \text{ in} = 192 \text{ in-k} \quad (3)$$

Based on the loading diagram presented in Figure 6, the applied load to result in a 192 in-k moment is:

$$M = \frac{P_{\text{applied}}}{2} \times 30 \text{ in} \quad (4)$$

$$P_{\text{applied}} = \frac{M}{15 \text{ in}} = \frac{192 \text{ in-k}}{15 \text{ in}} = 12.8 \text{ kips} \quad (5)$$

It is apparent in comparing this load to the failure loads presented in Table 6 that all specimens exceeded the yield moment, indicating all tension reinforcement had yielded at the maximum load. For the UHPC specimens, repeating the same calculations with the measured ultimate strength of the No. 4 reinforcing bars, of 102 ksi (see Table 3) indicates that the bars would be expected to rupture at an applied load of 21.8 kips. Interestingly, four of five specimens exceeded this capacity, and none failed due to bar rupture. For the VHPC specimens, the measured ultimate strength of the No. 4 reinforcing bars was 109.5 ksi (see Table 3), indicating that the bars would be expected to rupture at an applied load of 23.4 kips. With four of the six test specimens exceeding this capacity, only one failed due to bar rupture.

#### 4.2.2. *Load vs. Displacement*

The load vs. deflection behavior of the specimens with No. 4 bars is shown in Figure 19, Figure 20, and Figure 21. For the UHPC, specimen U-4-3-I failed at the lowest load and specimen U-4-5-II failed at the highest load. However, in terms of ductility specimens U-4-5-I-E and U-4-6-I-E had the best response. For these beams, the displacement was increasing with no significant increase in load, so the tests were stopped before any bar slip was noted. The specimen with the shortest splice length, specimen U-4-3-I with 3 in splice length had the poorest performance. As seen in the load vs. deflection plots, the curve for U-4-3-I drops off before any significant inelastic behavior was observed. The sudden drop in load, with the significant increase in displacement and crack opening indicated reinforcement was slipping relative to the UHPC. In comparison the specimen with 4 in splice length, U-4-4-I, displayed inelastic behavior prior to failure although the reinforcing steel in tension also was deemed to be slipping relative to the UHPC. Beam U-4-5-II displayed the maximum capacity. Specimen U-4-5-II and specimen U-4-5-I-E had the same splice length and the same area of steel in tension. The difference between the two was the area of steel in compression. Specimen U-4-5-II was tested to ensure that the performance shown by U-4-5-I-E could be repeated even with the increase in the area of steel in compression.

For the VHPC, the specimens performed as expected. Specimen V-4-3-I failed at the lowest load and V-4-6-I failed at the highest load. Unlike the UHPC specimens, inelastic behavior was observed with all of the VHPC specimens. Specimens V-4-5-I and V-4-5-II both had a 5 in. splice length, with the same compression and tension reinforcement configuration. The large difference in ductility observed can be attributed to the extra VHPC present in the larger pocket for V-4-5-II. The larger pocket in specimen V-4-5-II allowed for the stress to increase enough to rupture the tension steel. To avoid having the VHPC pocket contribute more tensile strength than present in the previous tests where the pocket length was designed for the splice length, the final two specimens tested, V-4-3-I and V-4-4-I, had an initial crack cast into the VHPC pocket at the end of the both sides of the splice. This crack was created on both sides by placing a piece of cardboard at the end of the splice. This prevented the VHPC from carrying tensile stress across the face of what was the interface between the precast member and the pocket on the other specimens. In specimen V-4-5-II, which had a long pocket (15 in) but a short splice (5 in), the tension reinforcing steel ruptured at the interface of the precast member and the VHPC pocket rather than inside the pocket at the end of the splice.

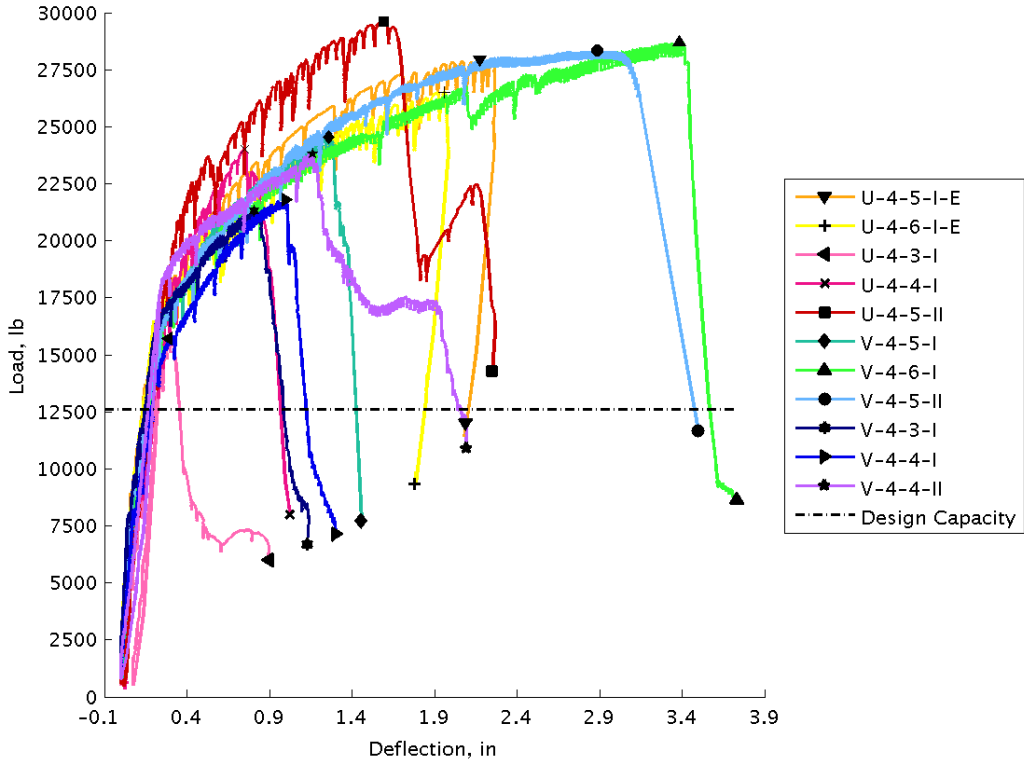


Figure 19. Load vs. South End Deflection for All Specimens with No. 4 Bars

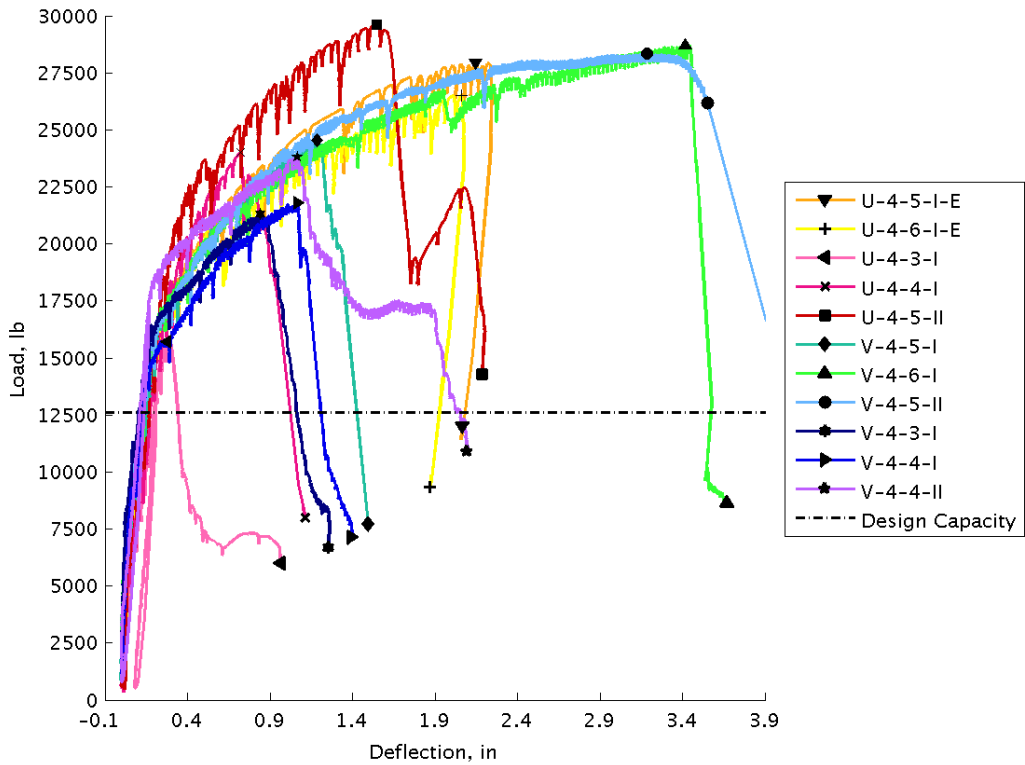
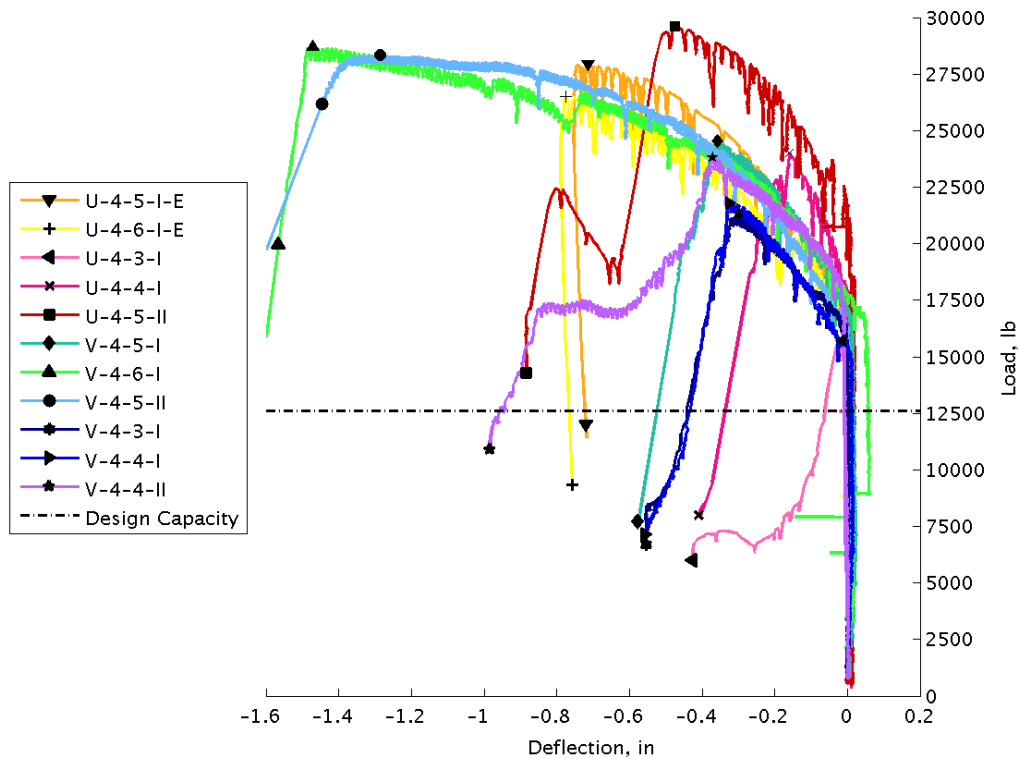


Figure 20. Load vs. North End Deflection for Specimens with No. 4 Bars



**Figure 21. Load vs. Midspan Deflection for Specimens with No. 4 Bars**

(note that upward displacement is negative).

Observing Figure 19 and Figure 20, the load vs. deflection plots show that the magnitude of deflection at the south end and the north end respectively was nearly equal, indicating that the spreader beam distributed the loads equally to both ends from a single actuator for all test specimens. In all specimens with No. 4 bars, the midspan did not show significant deflection until the specimens had cracked. Midspan deflections showed significant increases after the interfaces of the precast element and the pocket debonded.

#### 4.2.3. Load vs. Strain

The strains measured in the compressive reinforcement were plotted with respect to externally applied loads to observe the change in strains over the period of testing (shown in Figure 22 and Figure 23). The actuator load is plotted on the vertical axis. This is the load applied externally to the beam and not the load directly applied to the compressive reinforcing steel through flexure. Hence, the load vs. compressive strain plots do not represent the typical stress vs. strain behavior of a steel reinforcing bar.

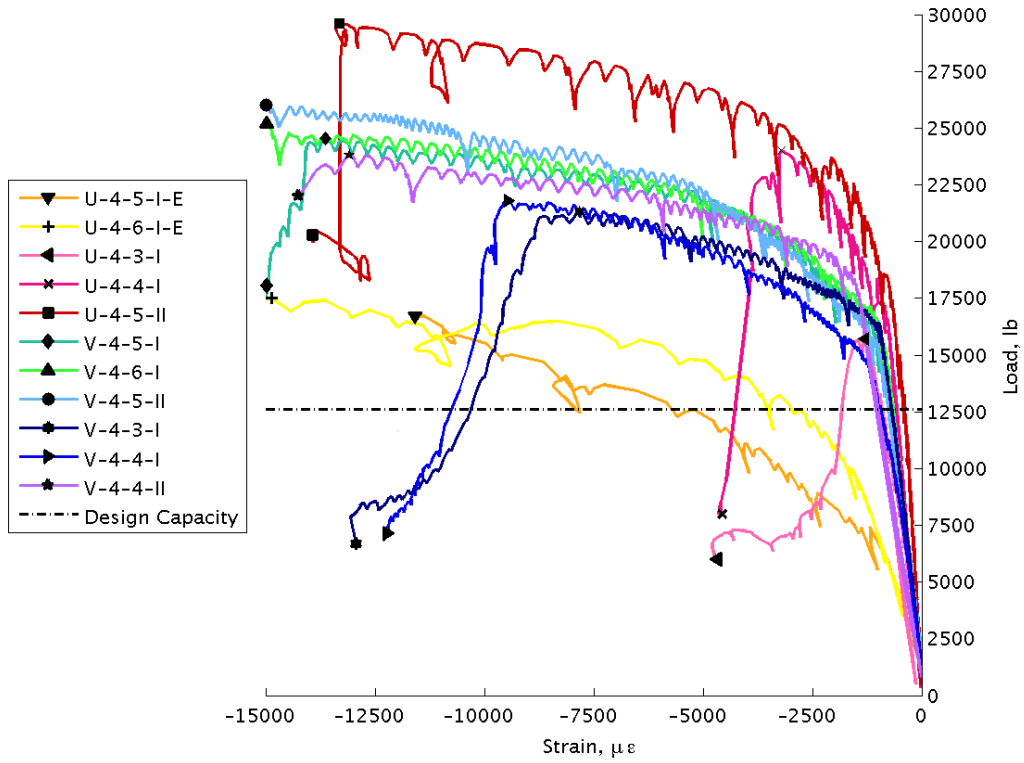


Figure 22. Load vs. Reinforcement Bar (East) Strain for Specimens with No.4 Bars

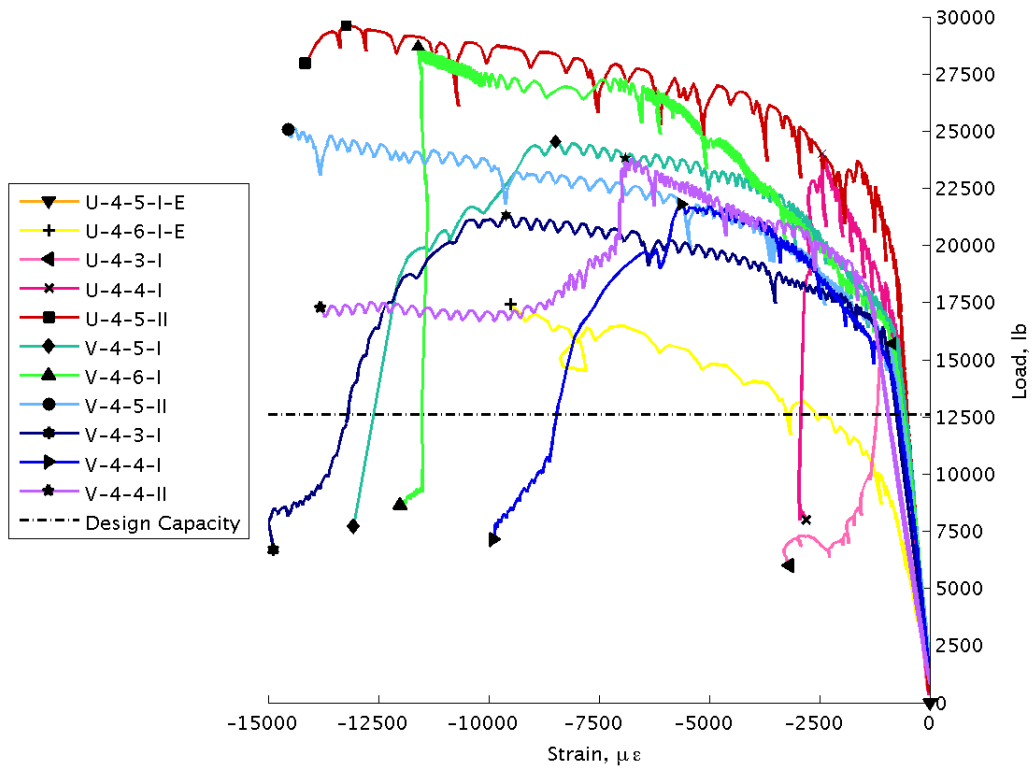
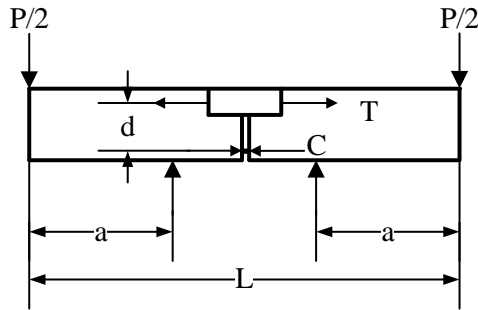


Figure 23. Load vs. Reinforcement Bar (West) Strain for Specimens with No. 4 Bars

Using a simple model, the force in the reinforcing steel in compression can be calculated as shown in Figure 24 and Equation 6.



**Figure 24. Force in Compressive Reinforcement from Externally Applied Loads**

From Figure 24,

$$C = \frac{P \times a}{2 \times d} \quad (6)$$

Based on this simplistic model, the compression reinforcement in the specimens with the larger amount of compression reinforcement (two No. 7 bars and one No. 6 bar or 2 No. 8 bars) should not have yielded. However, the strain gauges indicated that they did yield. This was because the strain gauges were placed on the bottom of the reinforcing bars, and the strain gradient through the bars was large enough that the bottom fibers of the bars did yield in compression while the top of the bar was in tension. This is discussed in greater detail in the Discussion section of this report.

From the load vs. strain plots in Figure 22 and Figure 23, the difference in behavior exhibited by the specimens with the smaller amount of compression reinforcement (U-4-5-I-E and U-4-6-I-E) and those with the larger amount of compression reinforcement is very noticeable. As would be expected, the smaller amount of compression reinforcement yielded at a much lower applied load. The compression reinforcement in Specimen U-4-3-I did not yield prior to achieving the peak load, due to the slipping failure of the tension reinforcement.

#### 4.2.4. Load vs. Interface Opening

The displacements at the interface of the precast element and the pocket were measured by LVDTs. Typically, the interface between the pocket and the precast concrete opened before any cracks were observed in the UHPC or VHPC pockets. After the interface opened completely, the crack would either propagate diagonally into the precast concrete below the pocket, or the interface would continue to debond along the bottom of the pocket. A schematic representation of the cracks in the precast element under the pocket is shown in Figure 25.

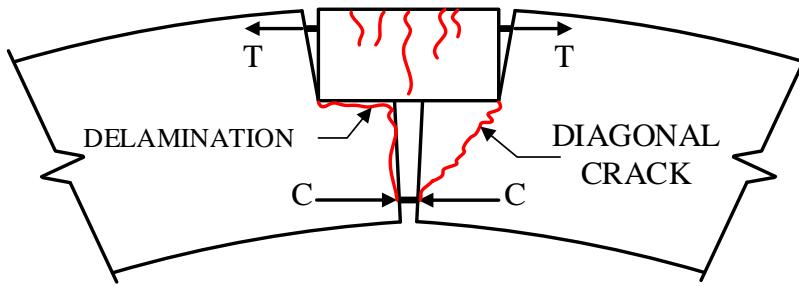


**Figure 25. Schematic Representation of Cracks in the Precast Element Under the UHPC Pocket**

The measurements were plotted with respect to the externally applied load as shown in Figure 26 and Figure 27. It can be observed that the load vs. interface displacement plots for all specimens are very similar prior to the interface debonding. After debonding the interface gaps at either end widened at different rates. Except for specimen U-4-3-I, all specimens showed evidence that the tension reinforcement had yielded and begun to strain harden. Slip is indicated when the gap opens considerably as the load drops off. Note that slip occurred at the south interface for most specimens, but at the north and south for specimen V-4-4-I.

The north interface of specimens U-4-5-I-E and U-4-6-I-E widened more than the south interface. Potentially, the reinforcement could have pulled out or ruptured at this end but both tests were stopped prior to the occurrence of failure.

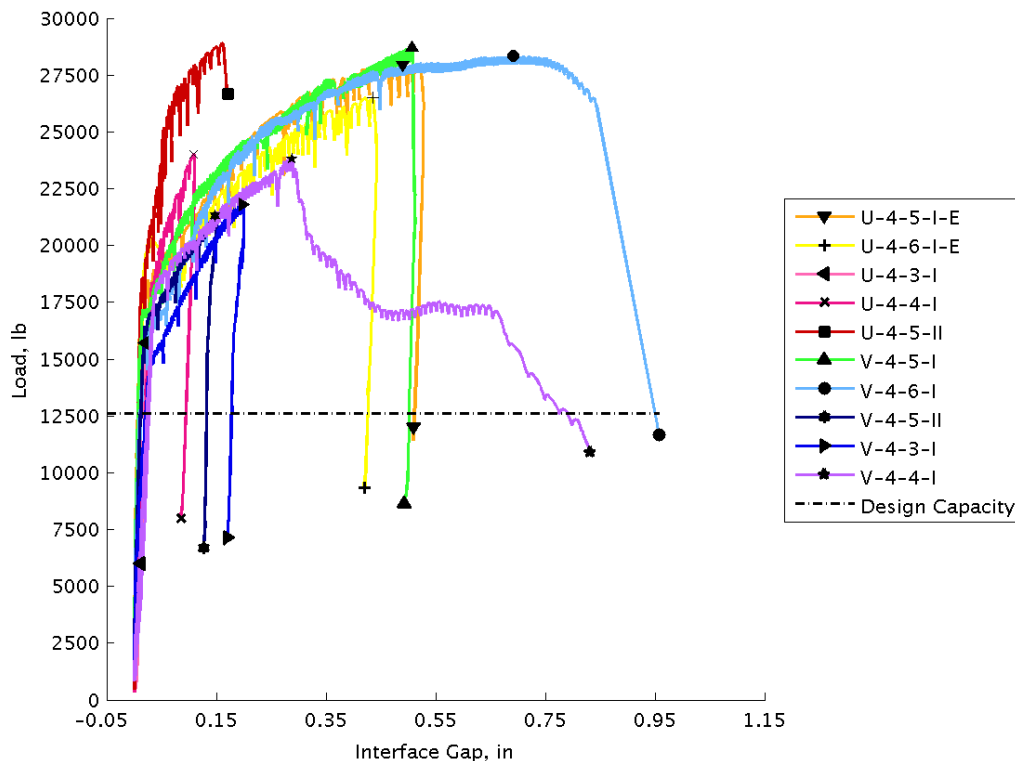


**Figure 26. Load vs. North Interface Displacement for Specimens with No. 4 Bars**

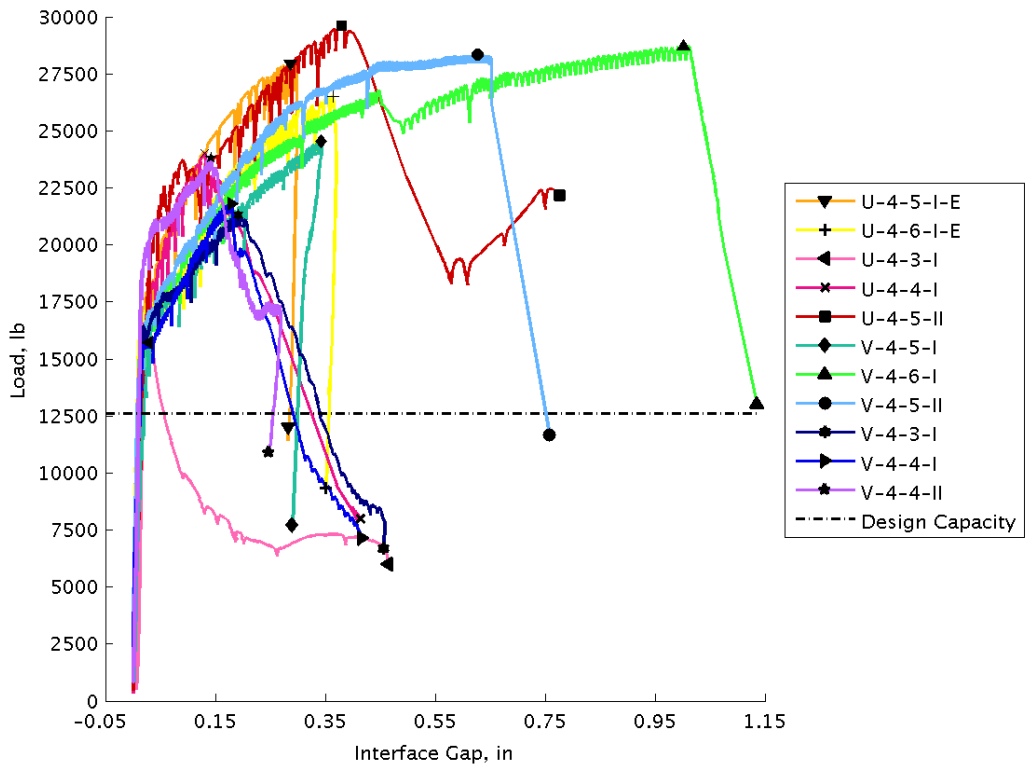


**Figure 27. Load vs. South Interface Displacement for Specimens with No.4 Bars**

#### 4.2.5. Load vs. DEMEC Strain Measurements

The surface strains were measured by a DEMEC gauge. Locations and designations of the locating discs for the DEMEC gauge are presented in Figure 28. DEMEC measurements of surface strain for Specimen U-4-5-I-E are shown in Figure 29. The surface strains confirm that in the specimens with No. 4 bars, most of the deformation in the beam occurred at one interface. The surface strains measured within the UHPC/VHPC pocket were very small as compared to the interface strains. The measurements can be easily understood by comparing the tensile strength of the UHPC/VHPC (typically around 1 ksi) to the bond strength of UHPC to precast concrete (typically around 0.3 ksi) and VHPC to precast concrete (typically around 0.2 ksi). Because the bond strength is lower, it can be expected that the interface will crack first in the region of constant moment. Once the interface cracks, the total tension force is carried across the interface by the reinforcing bar. Within the pocket, the tension force is shared by the reinforcing bar and the filler material up to the limiting strain. It is therefore expected that the strains within the pocket are much smaller than the strains across the interface.

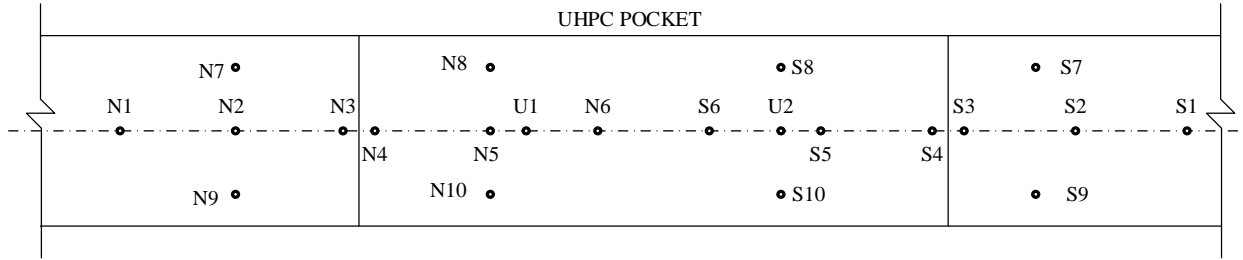


Figure 28. Locations and Designations of Locating Discs for DEMEC Gauge

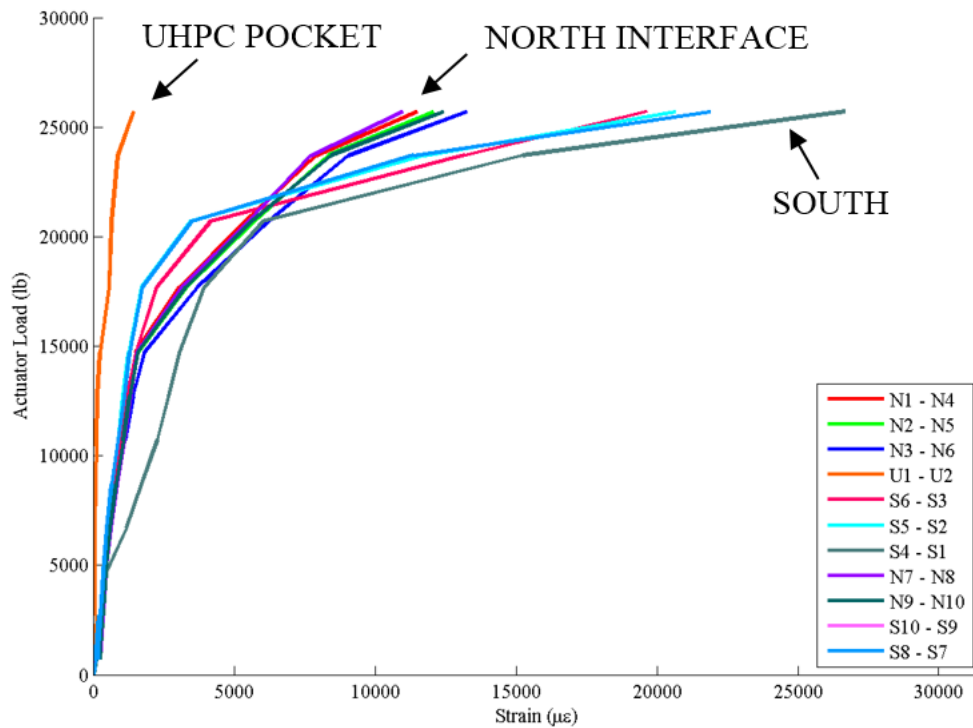


Figure 29. DEMEC Strain Measurements at the Top of the Beam for Specimen U-4-5-I-E

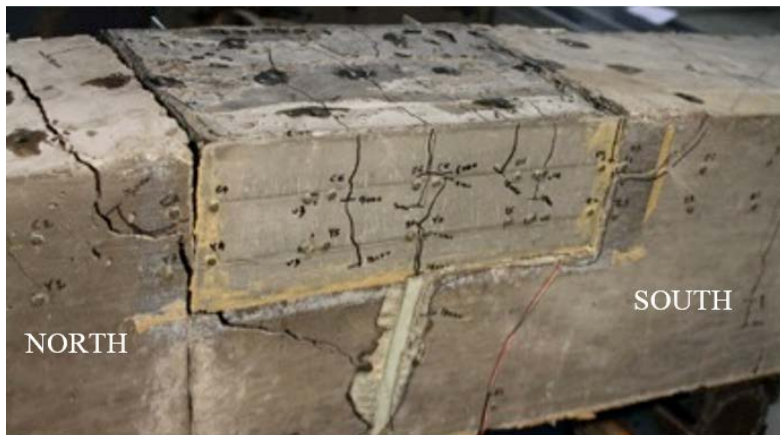
#### 4.2.6. Crack Patterns and Failure Modes

Figure 30 shows the UHPC pocket in specimen U-4-5-I-E which exhibited few flexural cracks. Most of the deformation occurred at the interface after the precast element and the UHPC pocket debonded. The flexural cracks in the UHPC pocket formed and propagated until the interface debonded. This behavior can also be seen in the load vs. surface strain relation plotted using the DEMEC measurements (Figure 29), which indicated the strains in the pocket were very small relative to the strains across the interfaces. The UHPC pocket did not show any signs of splitting cracks.



**Figure 30. UHPC Pocket in Specimen U-4-5-I-E Showing Interface Separation and Flexural Cracks**

Several flexural cracks can be observed in the UHPC pocket of specimen U-4-6-I-E at the time of failure (Figure 31). The UHPC pocket in U-4-6-I-E displayed more flexural cracks than specimen U-4-5-I-E. Splitting cracks were not observed in the UHPC pocket. The overall observed cracking pattern and the behavior were very similar to beam U-4-5-I-E.



**Figure 31. UHPC Pocket in Specimen U-4-6-I-E at End of Load Application Showing Flexural Cracks**

Specimen U-4-3-I did not show any flexural cracks at failure (see Figure 32). The predominant cracking observed was at the interfaces and at the corners of the UHPC pocket. Splitting cracks were observed prior to failure and only these continued propagating until the reinforcing bars slipped. The slip occurred at the south interface, as illustrated in Figure 27 by the gap widening considerably as the load dropped off.

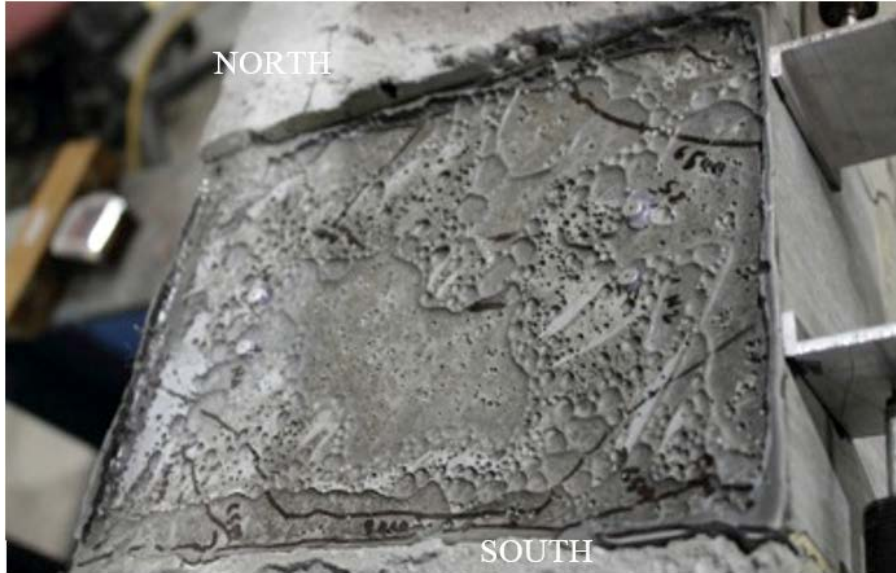


**Figure 32. UHPC Pocket in Specimen U-4-3-I Showing Cracks Near the Interfaces and the Corners**

Several flexural and splitting cracks could be observed in specimen U-4-5-II (see Figure 33). Flexural cracks occurred and propagated until a total applied load of 20,000 lb. Splitting cracks in the UHPC pocket started forming at loads over 20,000 lbs, and propagated until failure. The south interface cracked at about 15,000 lbs and widened until failure. The failure occurred after reinforcing bars at south interface slipped relative to the UHPC pocket. Most of the splitting cracks were concentrated near the south interface.



**Figure 33. UHPC Pocket in Specimen U-4-5-II After Failure Showing South Interface Separation**

In specimen U-4-4-I the flexural cracks could be observed in the UHPC pocket over the location of the foam block-out (see Figure 34). Some splitting cracks were observed at the south interface at loads above 23,000 lbs. Failure occurred after reinforcing bars slipped relative to the

UHPC pocket at the south interface. Flexural cracks stopped forming and propagating in the UHPC pocket after the interfaces debonded, as also seen in U-4-5-I-E and U-4-6-I-E tests.

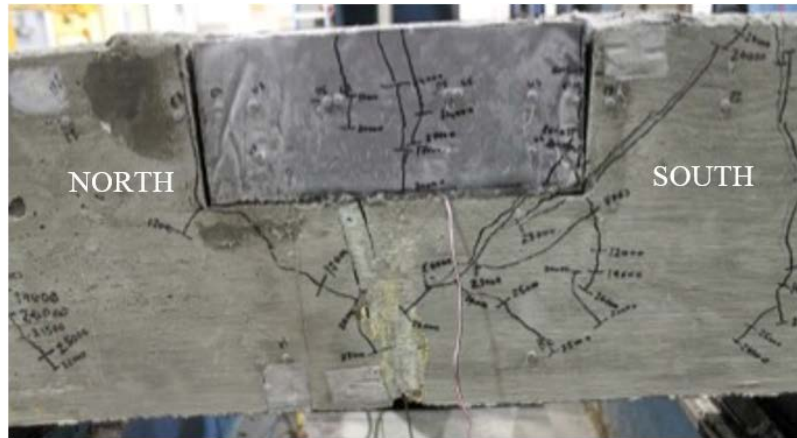


**Figure 34. Side View of UHPC Pocket in Specimen U-4-4-I After Failure Showing Interface Separation**

In specimen V-4-5-I, large splitting cracks formed on top of the VHPC pocket above both the east and west reinforcing bars at the north interface at 12,000 lbs (see Figure 35). This crack propagated downward towards the foam pad at midspan. These splitting cracks indicate that the reinforcing bars extending from the precast into the pocket at the north end of the member slipped relative to the VHPC pocket. This slip led to the specimen failure at 24,500 lbs.



**Figure 35. VHPC Pocket in Specimen V-4-5-I Showing Interface Separation and Splitting Cracks**

The cracking pattern of specimen V-4-6-I was very similar to specimen V-4-5-I. The main difference was that the main crack formed at the south end instead of the north (see Figure 36). The splitting cracks formed at 19,500 lbs and the specimen failed at 28,700 lbs. At the peak load, the south gap opened to over 1 in in width. At this time, the load dropped off suddenly, indicating the bars were slipping.



**Figure 36. VHPC Pocket in Specimen V-4-6-I Showing Interface Separation and Splitting Cracks**

Specimen V-4-5-II failed due to the reinforcing bars rupturing (see Figure 37). Cracks formed at the interface around the entire pocket at 1,500 lbs. The pocket continued to separate until the north face was completely detached. The reinforcing bars ruptured at 28,300 lbs causing the specimen to fail (see Figure 38).



**Figure 37. VHPC Pocket in Specimen V-4-5-II Showing Interface Separation and Reinforcing Bars Ruptured**



**Figure 38. Specimen V-4-5-II at End of Load Application Showing the Reinforcing Bars Ruptured**

Specimen V-4-4-II initially separated at the south interface and then formed a splitting crack on the east side of the pocket at the height of the reinforcing bars (see Figure 39). This splitting crack continued into the precast member at the same level, indicating that the reinforcing bar slipped both in the precast element and the VHPC pocket.



**Figure 39. VHPC Pocket in Specimen V-4-4-II Showing Interface Separation and Splitting Cracks**

Similar to specimen V-4-4-II, specimen V-4-3-I also had an initial splitting crack form on the east side of the VHPC pocket at the artificial south interface (see Figure 40). This indicates that there was also some slipping of the reinforcing bar within the VHPC pocket.



**Figure 40. VHPC Pocket in Specimen V-4-3-I at End of Load Application Showing Interface Separation**

Specimen V-4-4-I did not exhibit many cracks within the VHPC pocket (see Figure 41). Instead, the artificial south interface widened and the specimen failed at 21,800 lbs.



**Figure 41. VHPC Pocket in Specimen V-4-4-I at End of Load Application Showing Interface Separation**

In summary, all of the specimens in this series exhibited behavior and carried loads indicating that the tension reinforcing bars had yielded. The exact stress and strain in the tension bars at failure could not be measured directly. The next step in the data analysis is to indirectly determine the tension bar stress and strain based on the measurement of loads and compression bar strains. This analysis is presented in the DISCUSSION section.

### 4.3. Splice Test Results with No. 6 Bars and UHPC Splice Pocket Filler

#### 4.3.1. Summary of Test Results

The splice lengths tested with No. 6 bars ranged from 5 in to 8 in As described previously, the tests were performed in two stages, with the first two tests having an equal area of compression and tension reinforcement (two No. 6 bars), and the second two tests having a greater amount of compression reinforcement (two No. 8 bars and one No. 7). The typical details are shown in Figure 2 and Figure 3. Table 7 presents the cracking load, maximum load measured for each specimen, and failure mode.

**Table 7. Test Results for Specimens with No. 6 Bars and UHPC**

Specimen Designation	Splice Length, in	Compression Reinforcement	First Cracking Load, kips	Maximum Load, kips	Failure Mode
U-6-5-I-E	5	2 No. 6s	7800	35,080	slip
U-6-6-I-E	6	2 No. 6s	8000	35,710	slip
U-6-7-I.	7	2 No.8s and 1 No. 7	9000	43,200	slip/split
U-6-8-I.	8	2 No.8s and 1 No. 7	9300	43,480	slip/split

The nominal strength of the specimens was calculated based on the nominal yield strength of the tension reinforcement and the moment arm between the compression and tension reinforcement. For this basic calculation, the contribution of the UHPC to flexural strength is ignored.

$$A_s = 0.44 \text{ in}^2 \times 2 = 0.88 \text{ in}^2 \quad (7)$$

$$M_n = A_s f_y \times \text{moment arm} = 0.88 \text{ in}^2 \times 60 \text{ ksi} \times 8 \text{ in} = 422 \text{ in-k} \quad (8)$$

Based on the loading diagram presented in Figure 6, the applied load to result in a 422 in-k moment is:

$$M = \frac{P_{\text{applied}}}{2} \times 30 \text{ in} \quad (9)$$

$$P_{\text{applied}} = \frac{M}{15 \text{ in}} = \frac{422 \text{ in-k}}{15 \text{ in}} = 28.2 \text{ kips} \quad (10)$$

It is apparent in comparing this load to the failure loads presented in Table 7 that all specimens exceeded the yield moment, indicating all tension reinforcement had yielded at the instant of failure. Repeating the same calculations with the ultimate strength of the No. 6 reinforcing bars, of 102 ksi (see Table 3) indicates that the bars would be expected to rupture at an applied load of 47.8 kips. None of the four specimens exceeded this capacity, and none failed due to bar rupture.

Typically the first flexural crack in all specimens with No. 6 bars was in the precast element over the supports between applied loads of 7000 and 10,000 lb. The first UHPC crack in these specimens was between total applied loads of 10,000 and 15,000 lb. Another typically observed feature of all No. 6 specimens was the occurrence of splitting cracks in UHPC at higher loads. Moreover, at higher loads the propagation of splitting cracks was more prevalent than propagation of flexural cracks. Eventually, the failure mode for all No. 6 specimens was slip/splitting type failure.

#### 4.3.2. Load vs. Deflection

The load vs. deflection behavior of the No. 6 specimens is shown in Figure 42, Figure 43, and Figure 44. All specimens with No. 6 initially bars displayed very similar linear load vs. deflection behavior. The specimens with equal amounts of tension and compression reinforcement displayed non-linear behavior at lower loads than the specimens with the greater area of compression reinforcement. The specimens with greater compression reinforcement also failed at higher loads than those with equal areas.

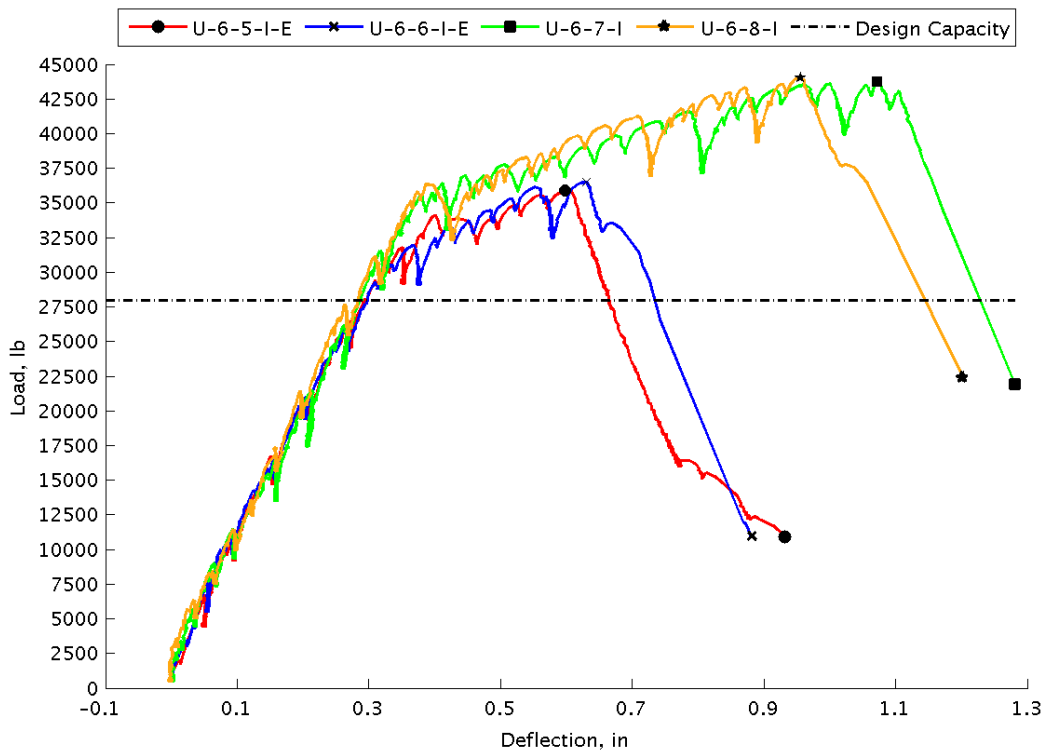


Figure 42. Load vs. South Deflection for All Specimens with No. 6 Bars

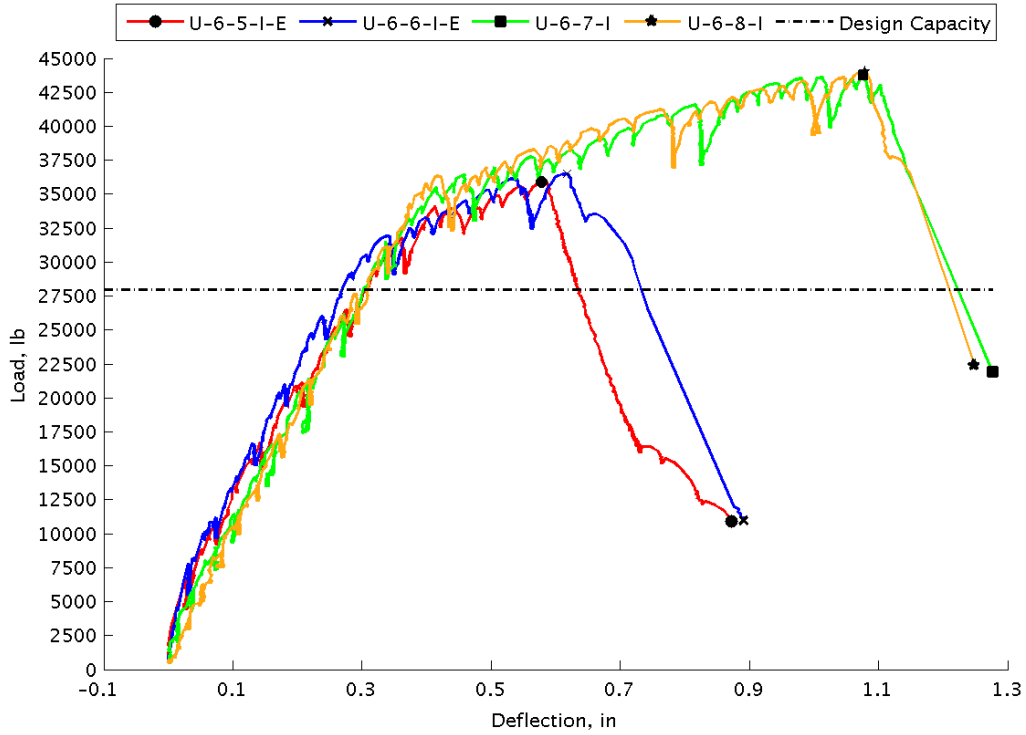


Figure 43. Load vs. North Deflection for All Specimens with No. 6 Bars

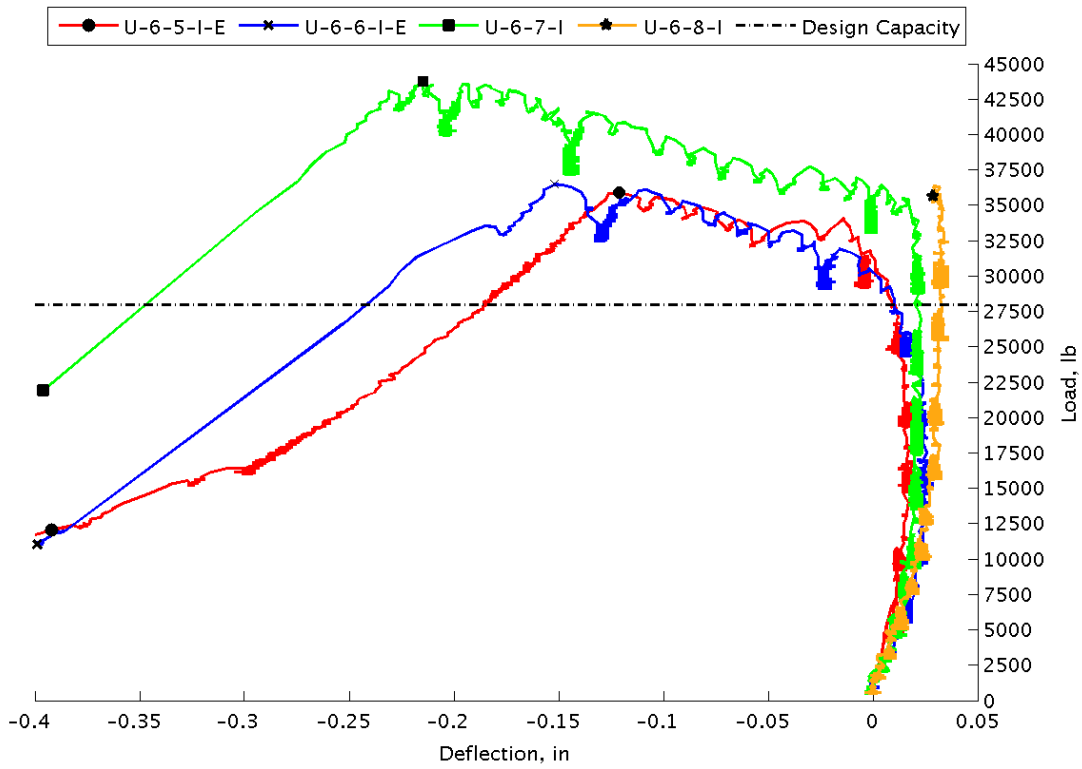


Figure 44. Load vs. Midspan Deflection for All Specimens with No. 6 Bars

(note upward deflection is negative)

The magnitudes of deflections at the north and south ends of all of the specimens were very similar, indicating that the actuator load was distributed equally by the spreader beam. The only time when any significant difference occurred was close to failure when the reinforcing bars on one side of the pocket slipped relative to the UHPC. The midspan deflections did not increase until the specimen had cracked significantly. The midspan deflections increased rapidly after the interface between the precast element and the UHPC pocket debonded.

#### 4.3.3. Load vs. Strain

The load vs. compressive strain plots for all specimens with No. 6 bars are shown in Figure 45 and Figure 46. The specimens which had an equal amount of tension and compression reinforcement (U-6-5-I-E and U-6-6-I-E) displayed non-linear behavior at lower loads than the specimens which had a greater amount of compression reinforcement (U-6-7-I and U-6-8-I).

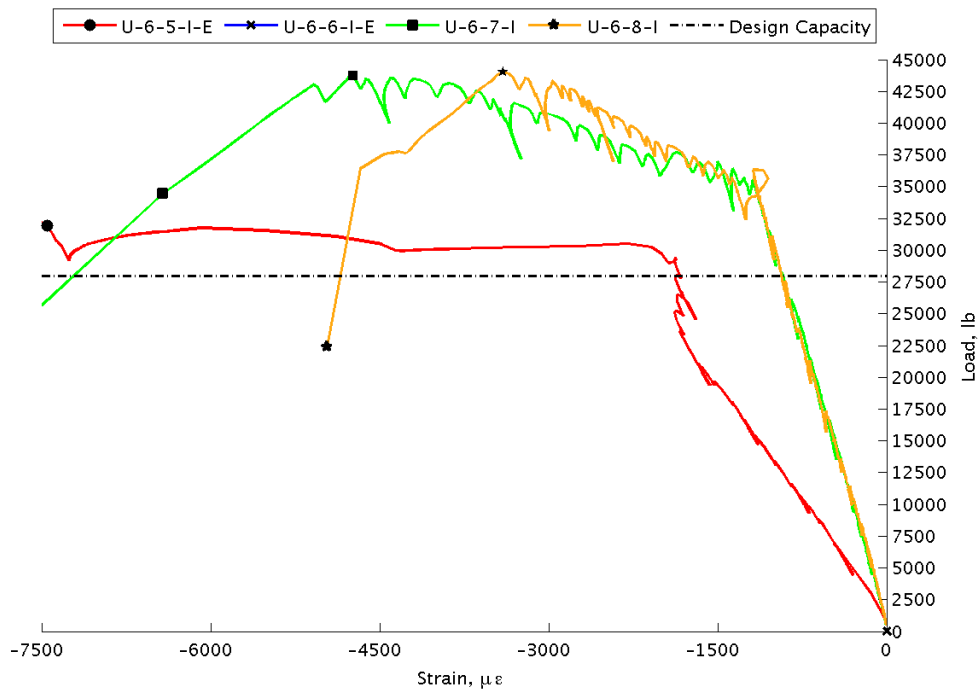
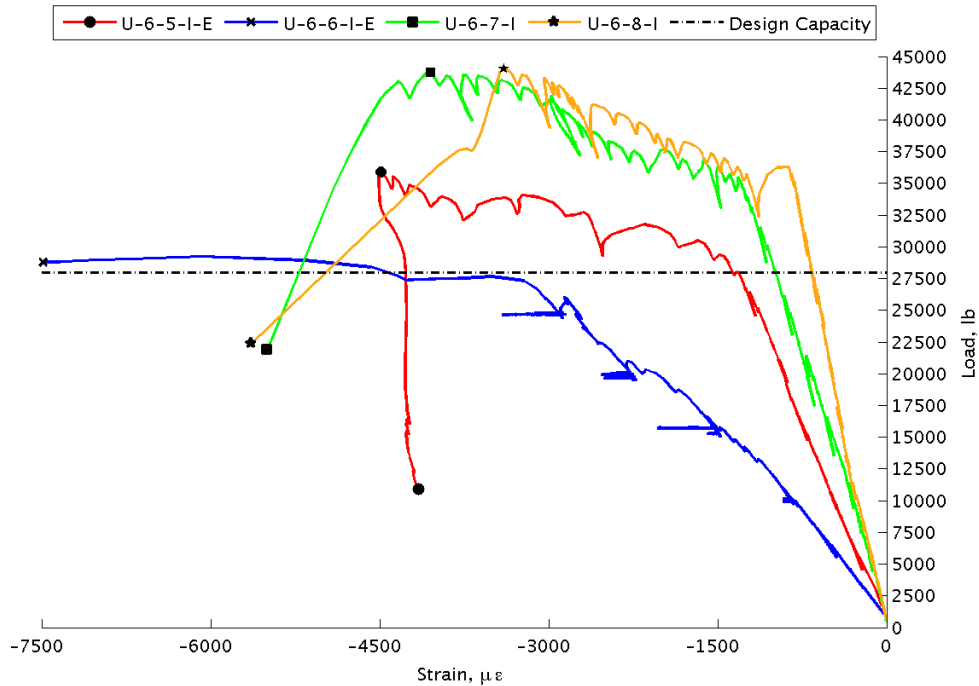


Figure 45. Load vs. Reinforcement Strain (East) for All Specimens with No. 6 Bars



**Figure 46. Load vs. Reinforcement Strain (West) for All Specimens with No. 6 Bars**

The loading on specimen U-6-5-I-E, albeit equal at north and south ends, was applied unsymmetrically on the specimen cross-section. This was not noticed during the loading and hence there was a substantial difference in the strains in the compressive reinforcement bars on the east side and the west side of the specimen cross-section. The strain gauge on the east reinforcing bar was possibly damaged during the concrete placement and was unable to record any strains during the test. The nature of unsymmetrical loading on U-6-5-I-E and only one working strain gauge on U-6-6-I-E caused the load vs. compressive strain plots of these specimens to be dissimilar. The strain increases were carefully monitored for specimens U-6-7-I and U-6-8-I, and unsymmetrical loading was avoided. Also, the overall increase in strain was much smaller in the specimens with the greater cross-sectional area of reinforcement in compression.

#### 4.3.4. Load vs. Interface Opening

The displacements at the interface of the precast element and the UHPC pocket are plotted in Figure 47 and Figure 48. Typically, cracks at the interface would become discernible after the applied load was above 15,000 lbs for all specimens with No. 6 bars. In specimen U-6-5-I-E the north interface cracked and widened at failure. The south interface did not undergo significant widening since the failure occurred due to slip of the reinforcing bars near the north interface. Similar behavior could be observed in specimen U-6-5-I-E, and the predominant widening of the interface occurred at the north interface. The displacements at the interface for specimens U-6-7-I and U-6-8-I were of similar magnitude until peak load was applied to the specimens. The displacements at the north and south interfaces of all specimens were unequal after the application of peak load.

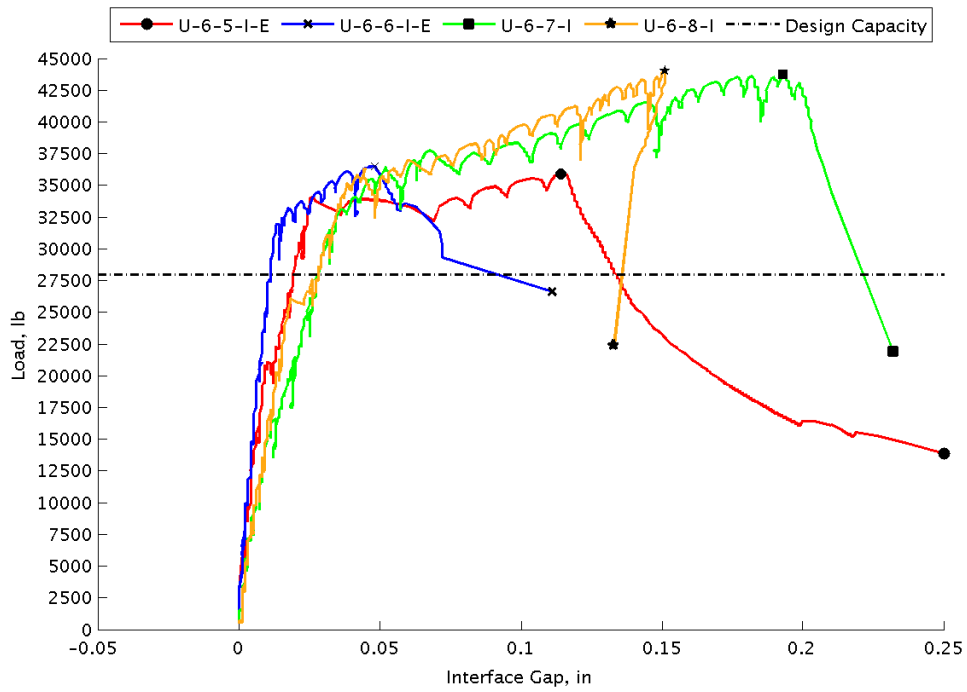


Figure 47. Load vs. North Interface Displacement for All Specimens with No. 6 Bars

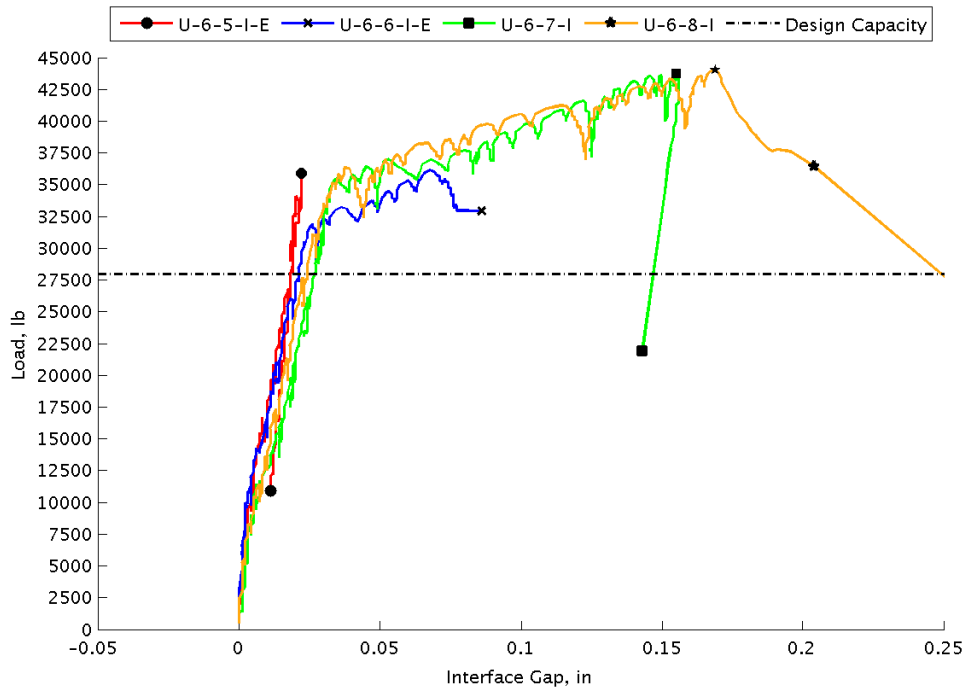


Figure 48. Load vs. South Interface Displacement for All Specimens with No. 6 Bars

It is noteworthy that in the specimens with equal tension and compression reinforcement, the interfaces that were closer to the roller support experienced the most deformation resulting in the widest gaps. However, the same behavior was not observed in the other two specimens. Moreover, an observation can be made that the values of interface displacement measured in all specimens with No. 6 bars at the peak were smaller than those measured in the specimens with No. 4 bars at the application of the peak load.

4.3.5. Load vs. DEMEC Strain Measurements

Figure 49 presents the surface strain measurements made with the DEMEC gauge at the top of the UHPC pocket for the specimen U-6-8-I. The numbering of the DEMEC points is as shown in Figure 28. The plot is typical for specimens with No. 6 bars. As seen in the specimens with No. 4 bars, the cracks, and hence the strains, at the interface were very large compared to the cracks within the UHPC pocket.

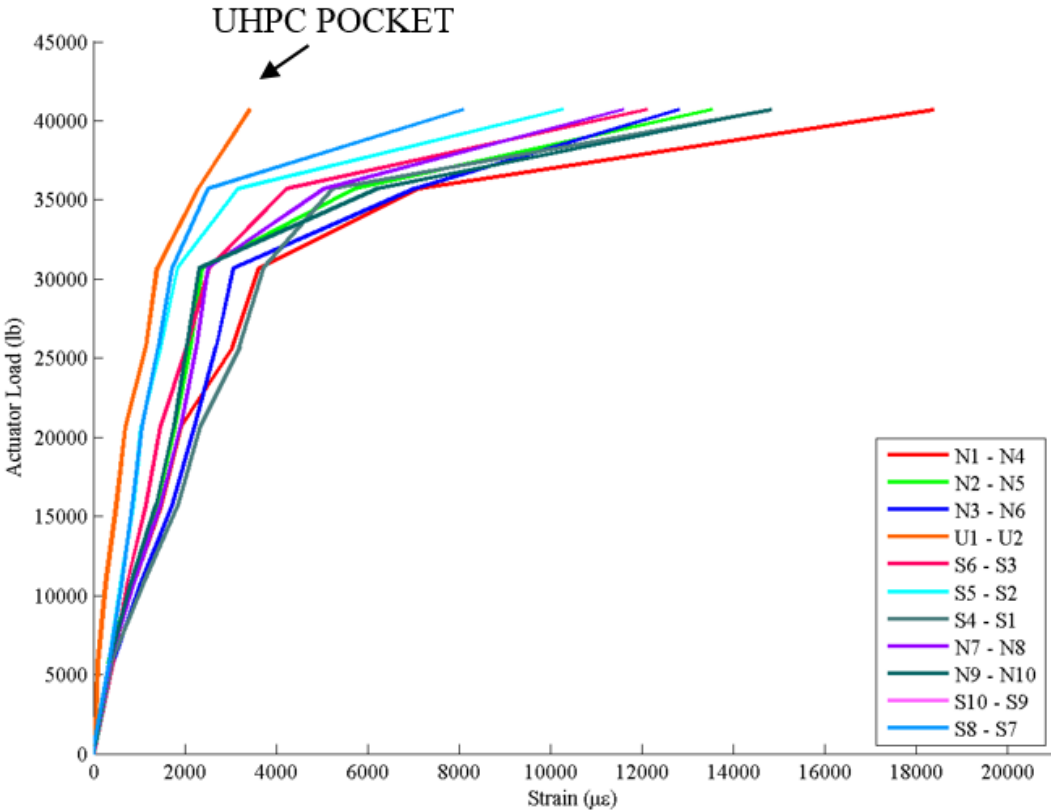
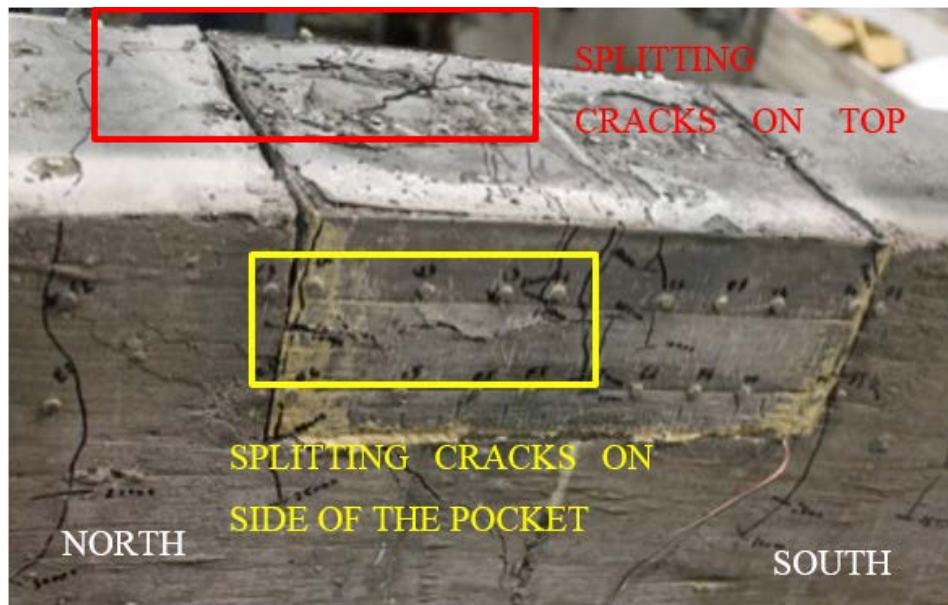


Figure 49. Strain Variation Observed at the Top of the UHPC Pocket in U-6-8-I

#### 4.3.6. Crack Patterns and Failure Modes

Throughout the testing program various failure modes were encountered. The significance of these failure modes is important to the discussion of the splice test results since several key conclusions can be made by observing the crack patterns in the UHPC pocket at failure.

Flexural cracks in the UHPC pocket of specimen U-6-5-I-E were observed at the midspan. Splitting cracks were observed at the north interface where the reinforcing bars appear to have slipped. As seen in Figure 50, splitting cracks can be observed at the top of the UHPC pocket predominantly closer to the eastern face which was the side with the higher load based on strain measurements. This crack was observed prior to failure and it opened up at failure. A single splitting crack was also observed at the depth of the reinforcing bar on the western face at the north interface. This crack occurred at the same instant that the specimen failed, and it may have been triggered by slipping of the reinforcing bars.



**Figure 50. Side View of the UHPC Pocket in Specimen U-6-5-I-E After Failure Showing Splitting Cracks**

Specimen U-6-6-I-E exhibited several flexural cracks during loading, and eventually the north interface separated. Prior to failure several splitting cracks were observed in the UHPC pocket over the location of the reinforcing steel. The eventual failure mode in this specimen was unique as compared to all specimens with No. 4 bars, but somewhat similar to the failure mode observed in specimen U-6-5-I-E. Splitting cracks occurred at the level of reinforcement and connected with the interface opening and the existing flexural cracks over the section with the foam. This mode of failure was caused by the short length of the splice reinforcement because the stiffness of the reinforcing bars projecting from the precast element and the splice bars was sufficient to precipitate splitting cracks and then separate the pocket into two parts. Essentially the short length of the reinforcement caused a “prying” action on the UHPC pocket as shown in Figure 51. The stiffness of the bars in the UHPC pocket was high enough to prevent the reinforcing bars from deforming with the UHPC in the pocket in a compatible manner.

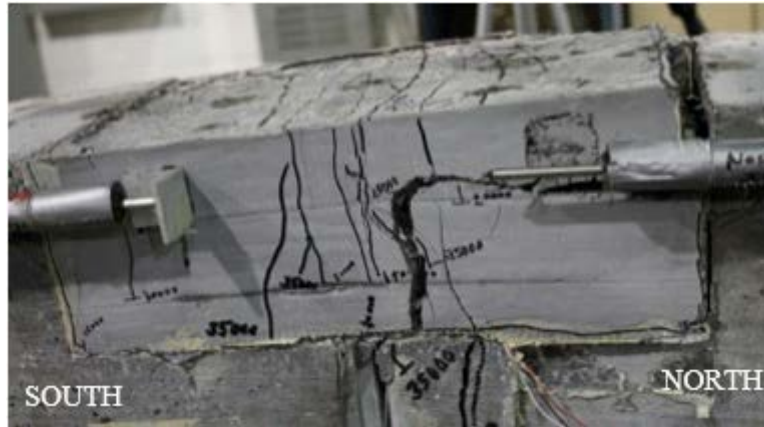


**Figure 51. Side View of UHPC Pocket in Specimen U-6-6-I-E After Failure Showing the Effect of Prying Action**

The failure mode of the specimens with the greater area of compression reinforcement was different as compared to the failure mode of the specimens with equal areas. Specimen U-6-7-I displayed several flexural cracks followed by splitting cracks in the UHPC pocket. The eventual failure was not at the interface as seen in previous specimens. Instead, the north interface began debonding prior to failure and the reinforcing bars projecting from the north into the pocket began to slip. At failure, as the bars projecting from the north slipped out, and an existing flexural crack widened. This flexural crack occurred at the tip of the splice bars and propagated at an angle to the beam axis, close to the bars projecting from the north. The failure mode and associated cracking can be seen in Figure 52. The width of the primary crack in the UHPC, compared to the opening of the north interface, indicate that at failure the bars projecting from the north slipped as the diagonal splitting crack developed.



**Figure 52. Top of the UHPC Pocket in Specimen U-6-7-I After Failure**

The failure mode of specimen U-6-8-I was similar to that seen in specimen U-6-7-I. An existing flexural crack widened at failure. In this case the location of the crack indicates that

failure was initiated between the bars projecting from the precast element into the UHPC pocket. The width of the crack also indicates that the splice bars slipped relative to the UHPC pocket. The failure mode of specimen U-6-8-I can be seen in Figure 53. The crack highlighted in Figure 53 occurred after applying an additional displacement increment to the specimen after failure.

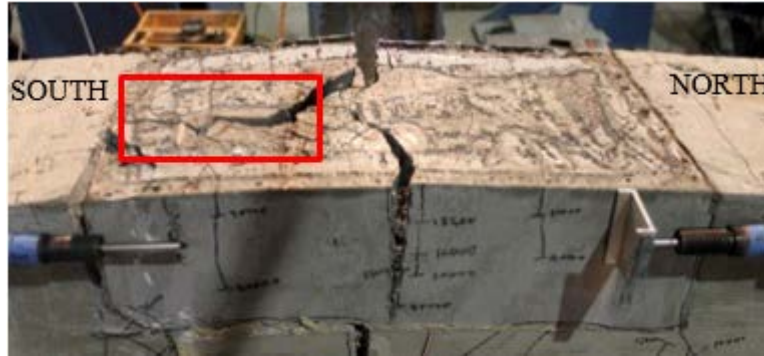


Figure 53. Specimen U-6-8-I After Failure

## 5. DISCUSSION

### 5.1. Summary of Strains in Compression Reinforcement

The principal answer sought in this testing was what splice length was sufficient to yield the uncoated No. 4 and No.6 reinforcing bars in the UHPC and VHPC pockets. The magnitude of strain in tension was not measured directly so the stress in the tension reinforcement must be determined indirectly. The strain in compression was measured in the tests via strain gauges and a summary of strains recorded at different loads during the test are presented in Table 8 and Table 9. The strains presented in these tables for each test are the average of the two values measured directly by strain gauges on the two extreme reinforcing bars in compression.

Table 8. Average Strain Gauge Measurements in Specimens with No. 4 Bars

		Load, lb	6000	12000	15000	20000	Peak
Equal Compr. Reinfor.	U-4-4-I-E	Strain Gauge Measurements, $\mu\epsilon$	-1315	-5993	-10755	NA	NA
	U-4-5-I-E		-905	-3144	-7030	NA	NA
Greater Compr. Reinfor.	U-4-3-I		-372	-811	-1097	NA	-3509
	U-4-4-I		-359	-596	-757	-1704	-3152
VHPC	U-4-3-I		-257	-473	-639	-1122	-4795
	V-4-5-I		-292	-632	-903	-2907	-11103
	V-4-6-I		-627	-987	-1177	-3305	-12382
	V-4-5-II		-728	-1141	-1541	-4144	NA
	V-4-3-I		-375	-764	-994	-6006	-399
	V-4-4-I		249	-227	-633	-4162	194
	V-4-4-II	-1849	-2339	-2585	-4367	-11426	

**Table 9. Average Strain Gauge Measurements in Specimens with No. 6 Bars**

	Equal Compr. Reinforcement		Greater Compression Reinforcement	
	U-6-5-I-E	U-6-6-I-E	U-6-7-I.	U-6-8-I.
Load, lb	Strain Gauge Measurements, $\mu\epsilon$			
6000	-436	-690	-212	-194
12000	-828	-1181	-410	-391
15000	-1033	-1560	-514	-465
20000	-1338	-2339	-690	-603
30000	-3449	-10382	-1079	-884
40000	NA	NA	-2905	-2503
Peak	-8047	NA	-7072	-9018

Based on material tests presented in Table 3, and the measured strains in Table 8 and Table 9, it is clear that all compression bars exceeded their yield strain at some point during testing. The specimens with a greater amount of compression steel than tension steel were not expected to yield, based on an average stress in the bars. However, the strain gauge was placed on the bottom of the bars, and there was a significant strain gradient through the depth of the bars. Therefore, even if the strain at the center of the bar was less than yield, the strain gage on the bottom of the bar could indicate yielding. To get a better understanding of the behavior of the cross-section, and thereby determine the forces in the spliced bars, a strain compatibility analysis was performed on the four tested cross-sections. The following section describes the assumptions made in the analysis.

## 5.2. Strain Compatibility Analysis

To perform a strain compatibility analysis, the constitutive relationships for each material must be known. For the reinforcing steel, the material properties determined during testing were averaged for all bar sizes to result in a single stress-strain relationship used for all bars. The relationship is presented in Figure 54, and the equations for various strain ranges are presented in Table 10.

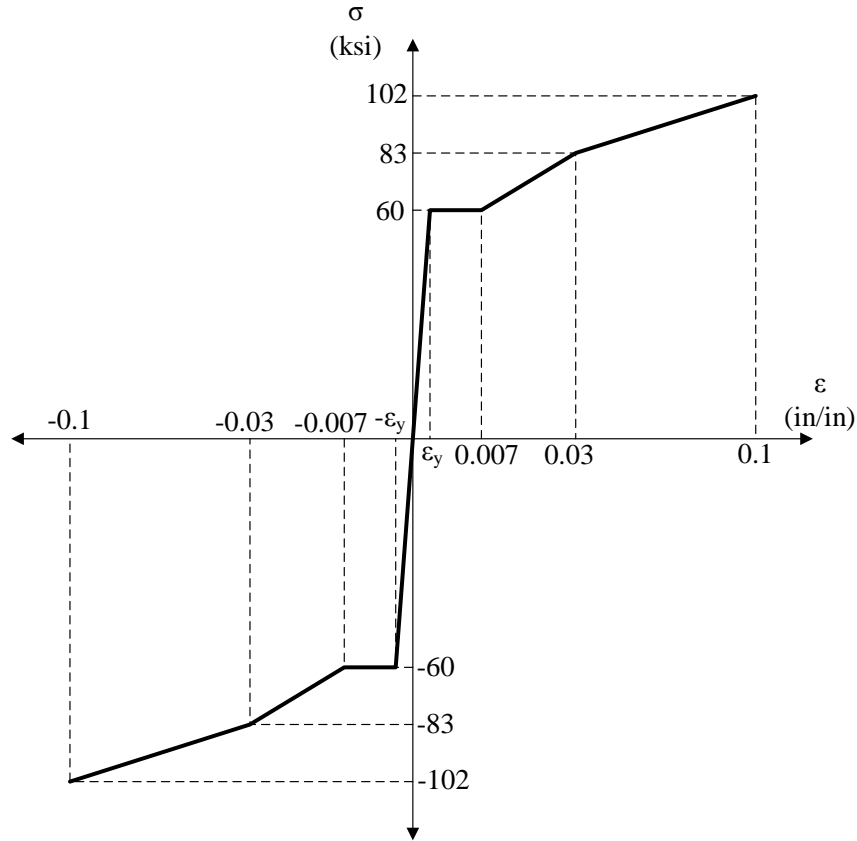


Figure 54. Stress-Strain Relationship for Reinforcing Steel

Table 10. Equations for Steel Stress and Strain

Strain Range	Equation
$\epsilon_s > 0.03$	$F_s = 85 + (\epsilon_s - 0.03)214 \leq 102$ ksi
$0.007 \leq \epsilon_s < 0.03$	$F_s = 60 + (\epsilon_s - 0.007)1087$
$\epsilon_y \leq \epsilon_s < 0.007$	$F_s = 60$
$-\epsilon_y \leq \epsilon_s < \epsilon_y$	$F_s = \epsilon_s E_s$
$-0.007 < \epsilon_s \leq -\epsilon_y$	$F_s = -60$
$-0.03 < \epsilon_s \leq -0.007$	$F_s = -60 + (\epsilon_s + 0.007)1087$
$\epsilon_s < -0.03$	$F_s = -85 + (\epsilon_s + 0.03)214 \geq -102$ ksi

Since the strain gradient for the cross-section at high loads was very steep, it was possible that part of the compression reinforcing bar could be yielded while the rest of the bar was elastic. At higher loads, it would be possible that part of the bar was strain hardening, while other parts were at yield. Therefore, a computational approach was needed to determine the total force in a bar, based on the strain distribution through the depth of the bar.

The approach adopted was to split the bar into 20 slices. For each slice, the location of the center of the slice relative to the center of the bar was calculated. Then, based on the curvature assumed for a given iteration, the strain at the center of each layer was calculated. Based on the relationships in Table 10, the stress in each layer was determined. The width of the layer was determined, and the area was calculated as the width of the layer times the thickness. This was not a precise calculation for the circular bar, but with 20 slices, was within 98% of the

actual area of each slice. Finally, the force in each layer could be calculated as the stress times the area, and all the forces were summed to determine the total force in the bar.

A constitutive model was also needed for the UHPC in the splice pocket. Figure 55 presents the model used, which was adopted from Russell and Graybeal (2013). For the UHPC in compression, the stress is simply the strain times the modulus of elasticity. On the tension side, the stress is the strain multiplied by the modulus up to the cracking stress. For strains larger than the cracking strain, but less than a limiting strain, the stress is assumed to be constant, and equal to the cracking stress. At strains larger than the limiting strain, the stress in the UHPC drops to zero.

The modulus, cracking stress and limiting strain were selected based on material tests, but there is some uncertainty related to these numbers. The analysis was performed using a high value for each parameter, and a low value. In this way, the behavior could be bracketed between two possibilities, one with very good UHPC performance and contribution to strength, and the other with lower performance. The lower performance standards are more similar to the interface between the UHPC and the concrete. This was the location that typically cracked first, and once cracked carried no tension. It is expected that the measured behavior would fall between these two extremes. The high and low values for the UHPC parameters are presented in Table 11. The same values were used for the VHPC.

**Table 11. Parameters for UHPC Constitutive Model**

Parameter	High Value	Low Value
Modulus of Elasticity	8000 psi	6000 psi
Cracking stress	1.0 ksi	0.25 ksi
Limiting Strain	0.010	0.0005

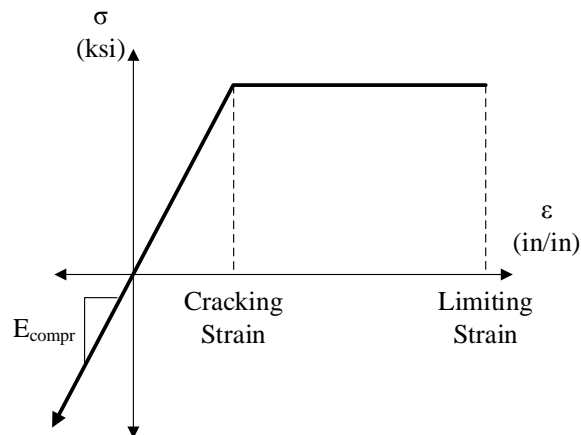


**Figure 55. Constitutive Model for UHPC and VHPC**

The calculations for the UHPC/VHPC pocket were also done by splitting the cross-section of the pocket into 20 strips of 0.25 in thickness. Based on the assumed curvature for a given iteration, the strain at the center of each strip was calculated. Then the stress and the force were calculated. To determine the internal moment, the centroid of the force in the UHPC/VHPC, relative to the top of the beam was also calculated.

The process to calculate one point on the load vs. strain-at-the-bottom-of-the-bar curve was as follows:

1. Select the strain at the centroid of the compression bar for the point to be calculated.
2. Select a neutral axis depth,  $c$ , measured from the center of the compression bar.
3. Based on strain and  $c$ , calculate the curvature,  $\phi = \epsilon/c$ .
4. Based on the strain and curvature, determine the strain at each layer of steel and UHPC/VHPC.
5. Based on strains and constitutive relationships, determine the stresses and forces in the UHPC/VHPC and steel bars.
6. Sum stresses, and iterate on  $c$ , until the forces sum to zero.
7. Based on  $c$ , calculate internal moment.
8. Based on internal moment and the statics of the beam specimens, calculate the externally applied load.

This process was repeated for increasing levels of strain at the center of the compression bar for four different cross-sections, representing the four combinations of compression and tension reinforcement tested in this program. For each cross-section, the analysis was done using the high and low values for the UHPC constitutive model shown in Table 11. Then, the calculated plots of load vs. strain-at-the-bottom-of-the-bar were compared to measurements from tests. The comparisons are shown in Figure 56, Figure 57, Figure 58 and Figure 59. The same calculations were performed for the VHPC specimens and the comparison of calculated vs. measured values is shown in Figure 60. Plots are shown for the analyses using the lower properties, because these calculations matched the measured values better.

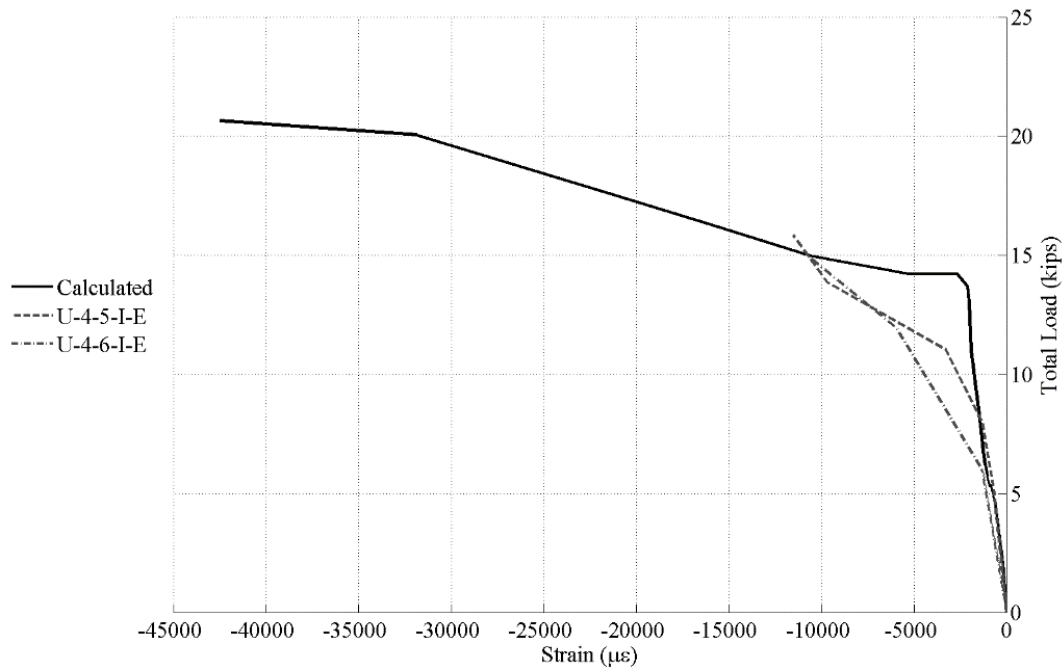


**Figure 56. Load vs. Strain at Bottom of Compression Reinforcement for Specimens with Two No. 4 Bars at Top and Bottom of Beam**

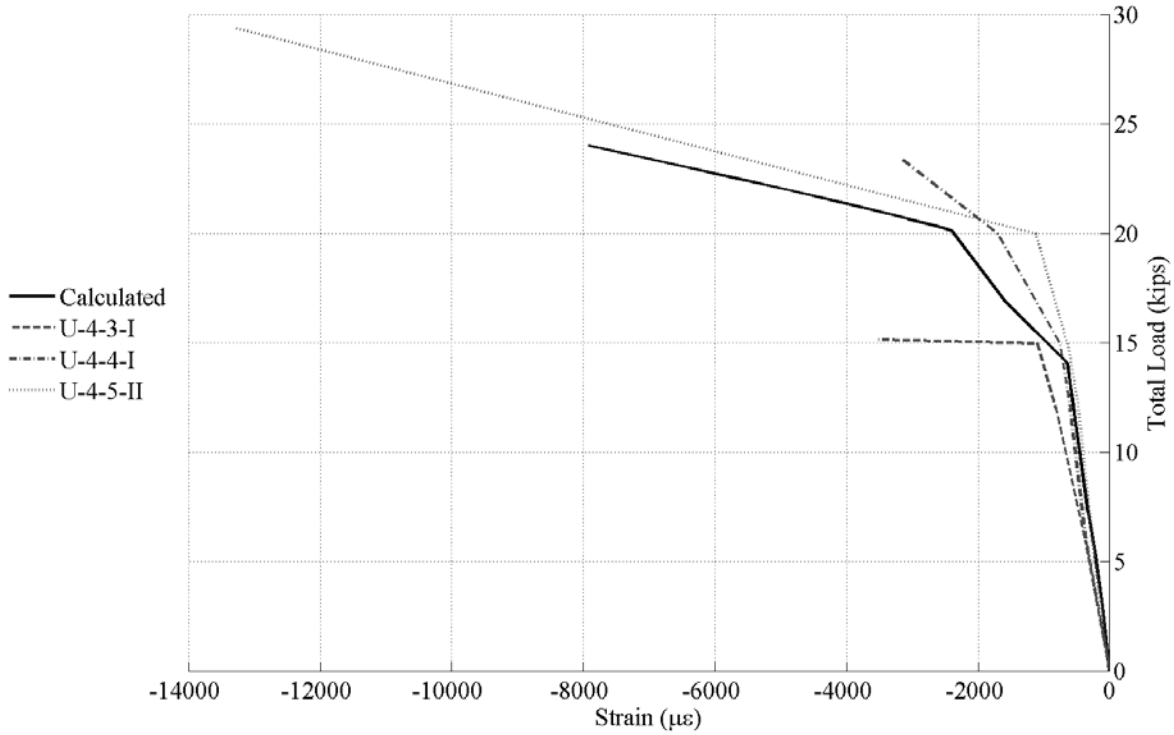


**Figure 57. Load vs. Strain at Bottom of Compression Reinforcement for Specimens with Two No. 4 Bars at Top and Two No. 7 Plus One No. 6 at Bottom of Beam**

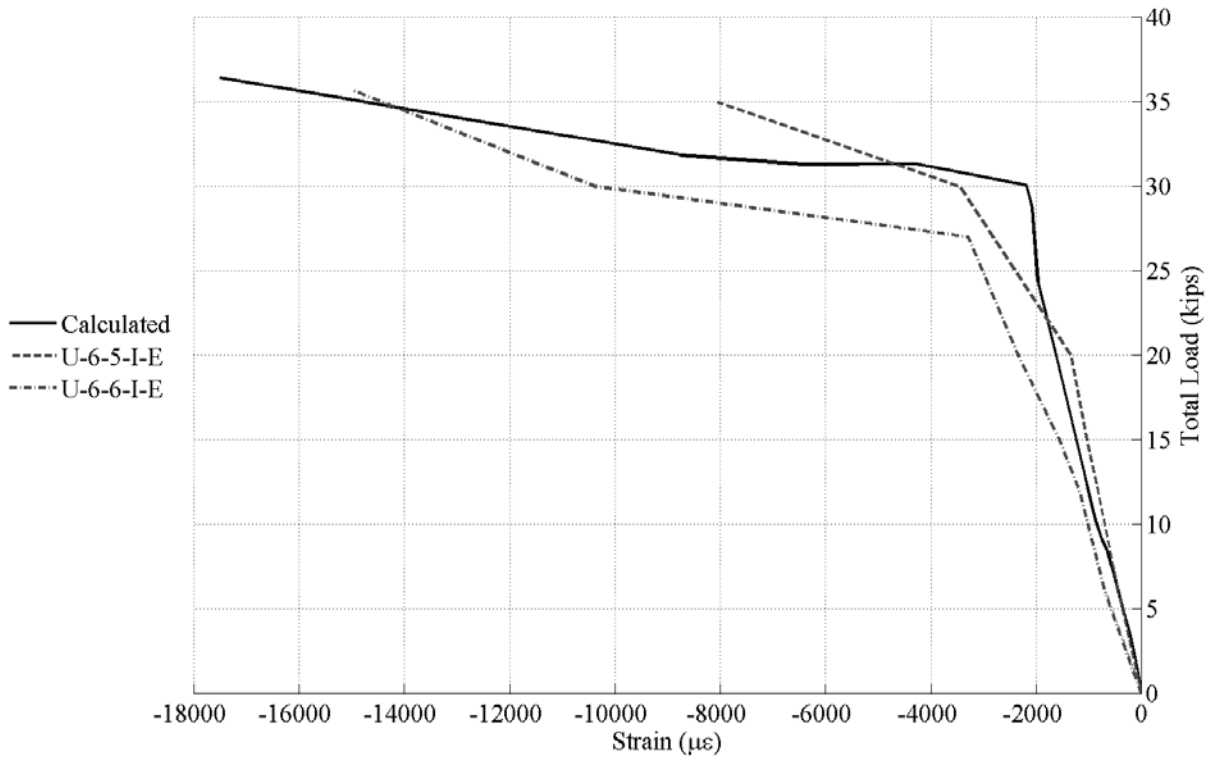


**Figure 58. Load vs. Strain at Bottom of Compression Reinforcement for Specimens with Two No. 6 Bars at Top and Bottom of Beam**

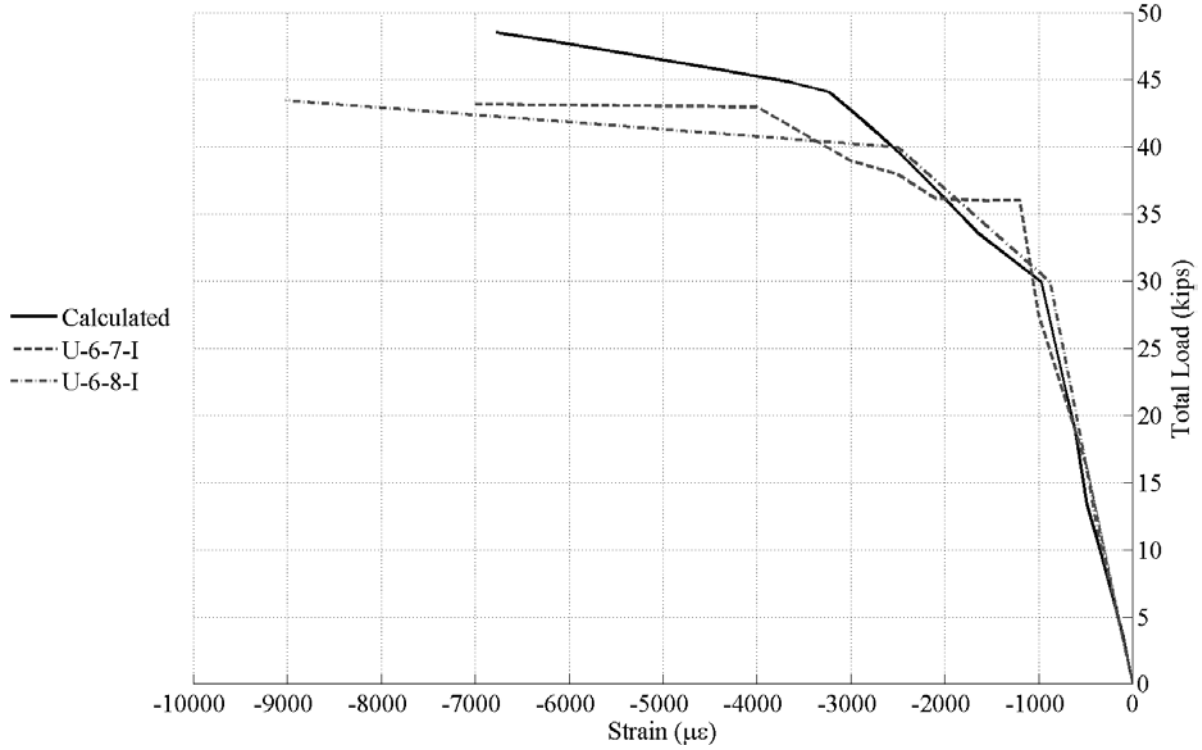


**Figure 59. Load vs. Strain at Bottom of Compression Reinforcement for Specimens with Two No. 6 Bars at Top and Two No. 8 Plus One No. 7 at Bottom of Beam**

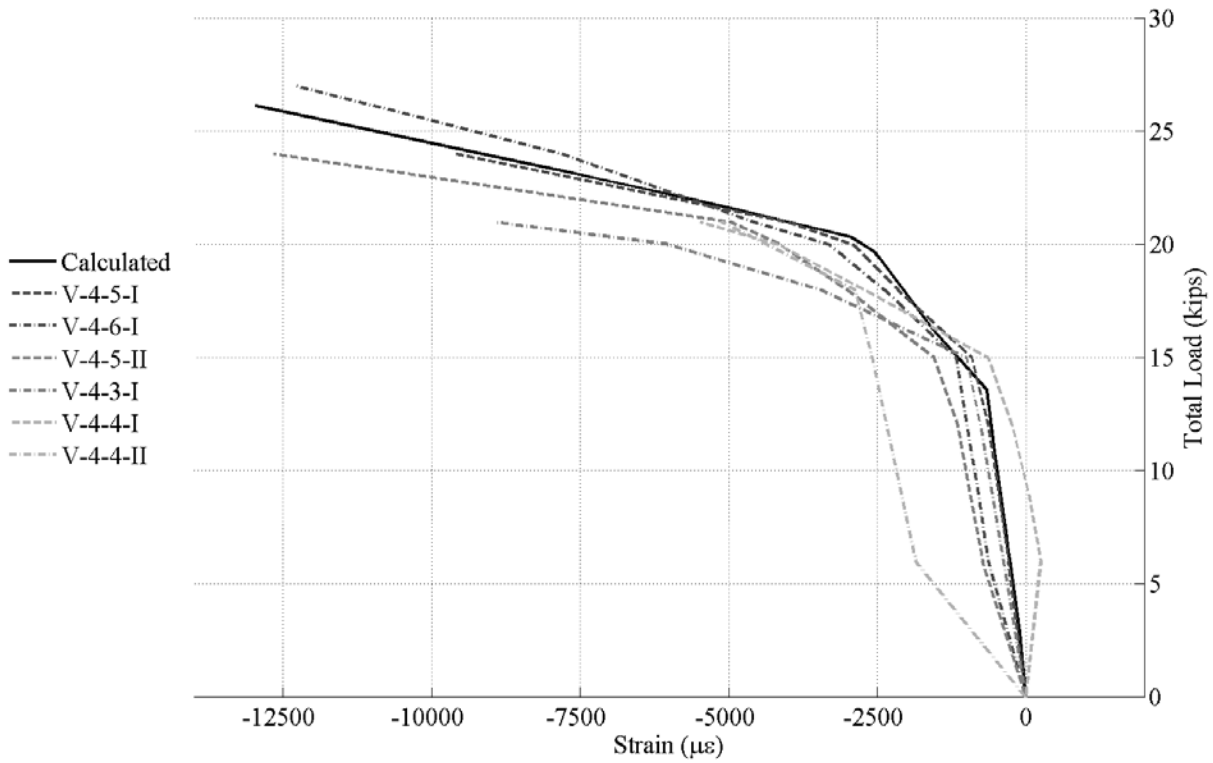


**Figure 60. Load vs. Strain at Bottom of Compression Reinforcement for Specimens with Two No. 4 Bars at Top and Two No. 8 at Bottom of Beam with VHPC**

Overall, a good agreement was observed between the strain compatibility analysis and the measured data. Differences between predicted and observed behavior were most likely caused by the averaging of steel material properties and the inherent variability in the bond strength between the pocket filler material and the concrete in the precast element.

Because the agreement between measured and calculated compression strains was good, the model was used to determine the strain in the tension reinforcement. For most specimens, the strain that was calculated for the tension reinforcement at the maximum measured compressive strain was selected as the maximum tension strain. For some specimens (U-4-5-II and U-6-8-I), the measured compressive strain was higher than predicted by the model. In this case, the model's maximum tension strain was selected to represent the maximum tested tensile strain. The scheme of selection of ultimate compressive strains is shown in Figure 61.

Based on the maximum tension strain determined from the analysis, the stress in the tension steel was calculated from the constitutive model shown in Figure 54. The strains and stresses in the tension steel were calculated and are reported in Table 12.

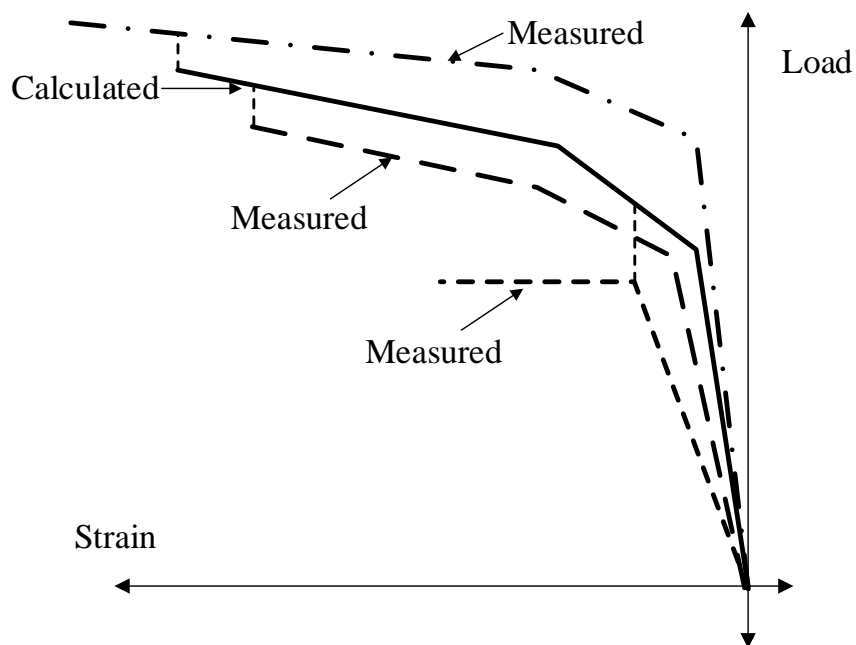


**Figure 61. Method for Selecting Strain in Compression Bars at Ultimate**

As observed in Table 12, the tension reinforcement in all specimens attained the yield stress. Therefore, based solely on the criteria of yield stress, a 3 in splice length is adequate for a No. 4 bar in UHPC or VHPC, and a 5 in splice length is adequate for a No. 6 bar in UHPC. However, ductility should also be considered. ACI 318-11 requires that for a beam to be

considered tension controlled, the tension reinforcement must reach a strain of at least 0.005, which was exceeded by all the specimens.

There are, however, several other factors that need to be considered in making the splice length recommendation. First is the inherent variability in construction. The actual splice length may be shorter than specified due to construction error, or there may be improper mixing or placing of the UHPC or VHPC around the splice which would reduce the bond strength. These possible problems would reduce the strength and ductility of the splice. The scope of this research project did not allow for multiple repetitions of splice lengths to be tested, so the inherent variability is unknown. Based on the expected variability in field splices, a 5 in splice is recommended for No. 4 bars and a 6 in splice is recommended for No. 6 bars, in UHPC or VHPC.

**Table 12. Maximum Strains and Stresses in Tension Reinforcement**

<b>Specimen Designation</b>	<b>Splice Length, in</b>	<b>Selected Strain in Compression, in /in</b>	<b>Maximum Strain in Tension Steel, in /in</b>	<b>Maximum Tension Stress, ksi</b>
U-4-5-I-E	5	0.012	0.010	63.3
U-4-6-I-E	6	0.011	0.009	62.2
U-4-3-I	3	0.001	0.016	69.8
U-4-4-I	4	0.003	0.040	87.1
U-4-5-II	5	0.008	0.100	100
V-4-5-I	5	0.008	0.110	102.3
V-4-6-I	6	0.008	0.140	108.6
V-4-5-II	5	0.008	0.145	109.5
V-4-3-I	3	0.008	0.104	100.8
V-4-4-I	4	0.005	0.066	92.6
V-4-4-II	4	0.005	0.062	91.8
U-6-5-I-E	5	0.008	0.008	60.9
U-6-6-I-E	6	0.015	0.013	66.5
U-6-7-I	7	0.007	0.067	92.9
U-6-8-I	8	0.007	0.067	92.9

## 6. CONCLUSIONS

Testing was performed to ascertain the performance of UHPC and VHPC as a filler material to allow the use of short splice lengths in longitudinal joints between adjacent box beam bridges. Based on the results of the static tests performed on simply supported beam specimens the following conclusions can be made:

1. Splice lengths with No. 4 bars of 3 in and longer were sufficient to yield the tension reinforcement prior to failure.
2. Splice length of No. 4 bars of 5 in is recommended to ensure ductility and allow for variability in construction.
3. Splice lengths with No. 6 bars of 5 in and longer were sufficient to yield the tension reinforcement prior to failure.
4. Splice length of No. 6 bars of 6 in is recommended to ensure ductility and allow for variability in construction.

## 7. REFERENCES

- Akhnoukh, Amin. *Development of High Performance Precast/Prestressed Bridge Girders*, Ph.D. dissertation, University of Nebraska, Lincoln, NE, 2008.
- Graybeal, B., *Material Property Characterization of Ultra-High Performance Concrete*, FHWA-HRT-11-038, Federal Highway Administration, Washington, DC, 2006.
- Graybeal, B. *Behavior of Field-Cast Ultra-High Performance Concrete Bridge Deck Connections under Cyclic and Static Structural Loading*, PB2011-101995, National Technical Information Service, Springfield, VA, 2010
- Graybeal, B. *Ultra-High Performance Concrete Composite Connections for Precast Concrete Bridge Decks*, PB2012-107569, National Technical Information Service, Springfield, VA, 2012.
- Perry, V. and Weiss, G. Innovative Field Cast UHPC Joints for Precast Bridge Decks- Design, Prototype Testing and Projects. *Proceedings of the International Workshop on Ultra High Performance Fibre Reinforced Concrete – Designing and Building with UHPFRC: State of the Art Development*, 2009.
- Perry, V.H. and Royce, M. Innovative field-cast UHPC joints for precast bridge decks (side-by-side deck bulb-tees), Village of Lyons, New York: Design, prototyping, testing and construction." *Proceedings of the 3rd fib International Conference*, Washington, DC, September, 2010.

Russell, H.G. and Graybeal, B.A. *Ultra-High Performance Concrete: A State-of-the-Art Report for the Bridge Community*, FHWA-HRT-13-060, Federal Highway Administration, Washington, DC, 2013.

Russell, H. G. (2009). *Adjacent Precast Concrete Box Beam Bridges: Connection Details. A Synthesis of Highway Practice*. United States: 86p.

8. APPENDIX

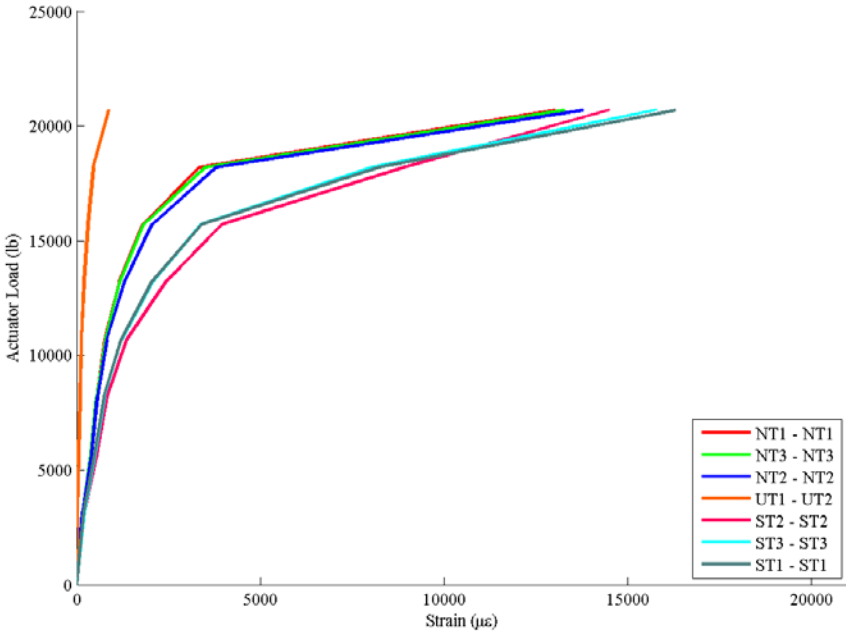


Figure 62. Strain Variation Observed at the Top of the UHPC Pocket in U-4-5-I-E

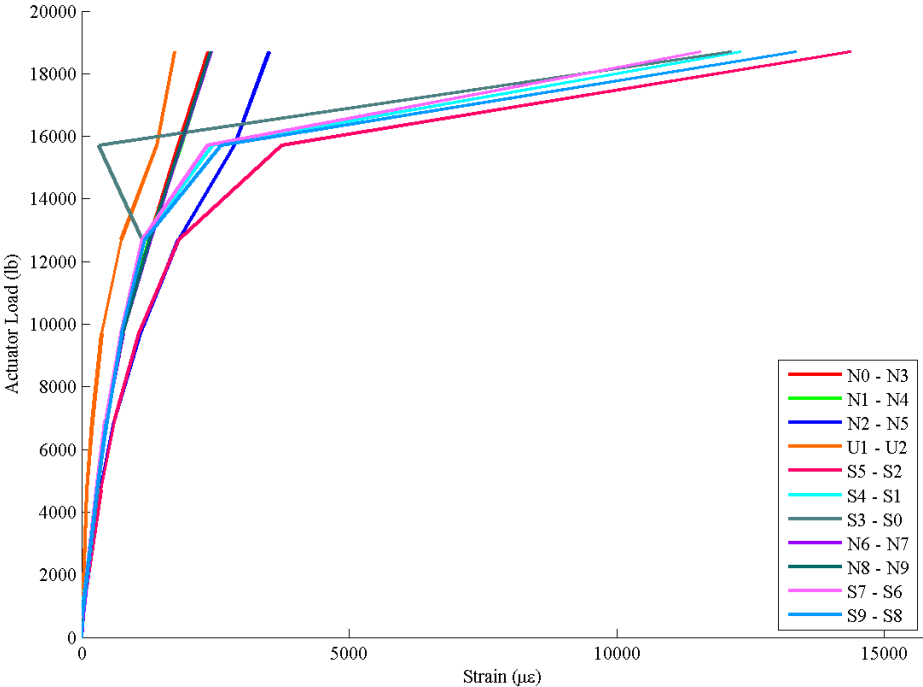
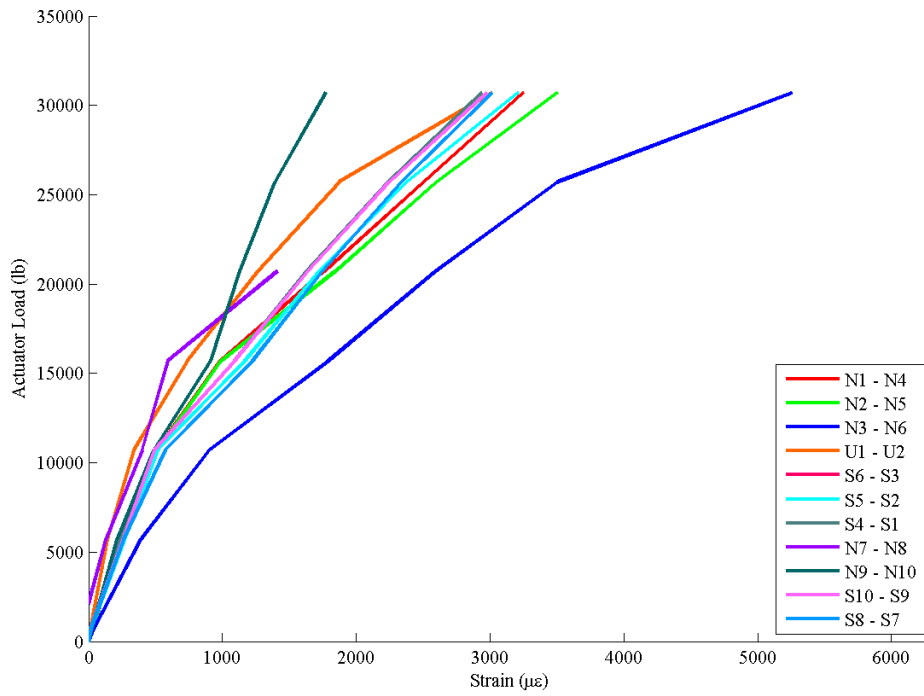
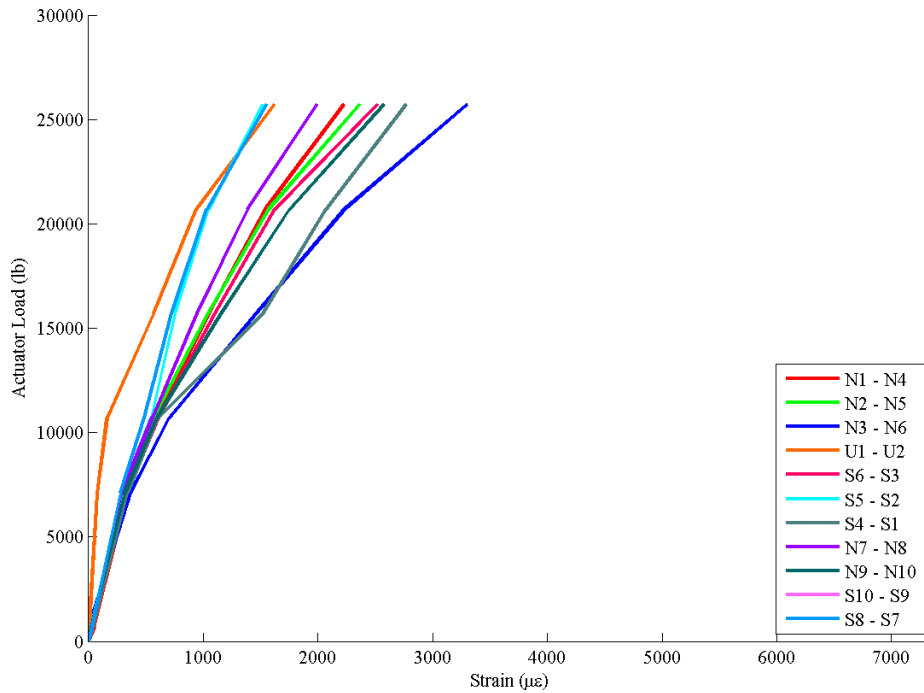


Figure 63. Strain Variation Observed at the Top of the UHPC Pocket in U-4-6-I-E



**Figure 64. Strain Variation Observed at the Top of the UHPC Pocket in U-4-3-I**



**Figure 65. Strain Variation Observed at the Top of the UHPC Pocket in U-4-4-I**

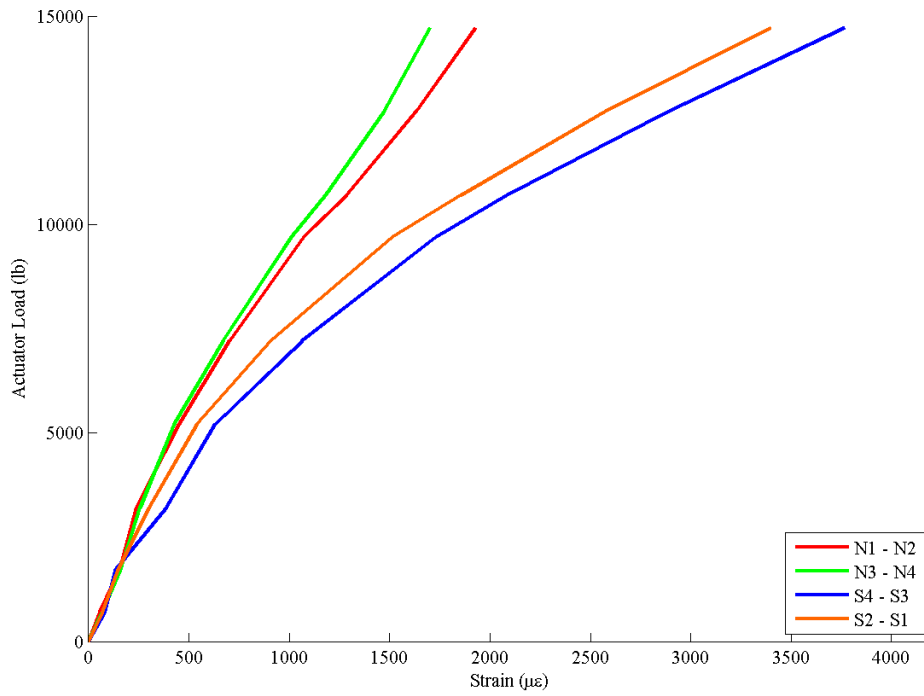


**Figure 66. Strain Variation Observed at the Top of the UHPC Pocket in U-4-6-I-E**

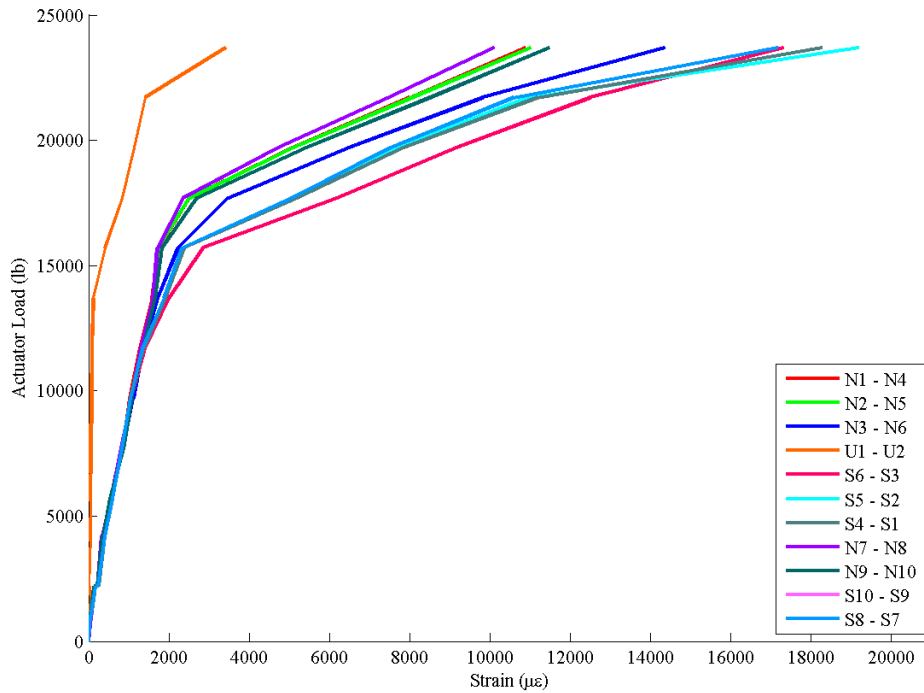


**Figure 67. Strain Variation Observed at the Top of the UHPC Pocket in U-6-5-I-E**

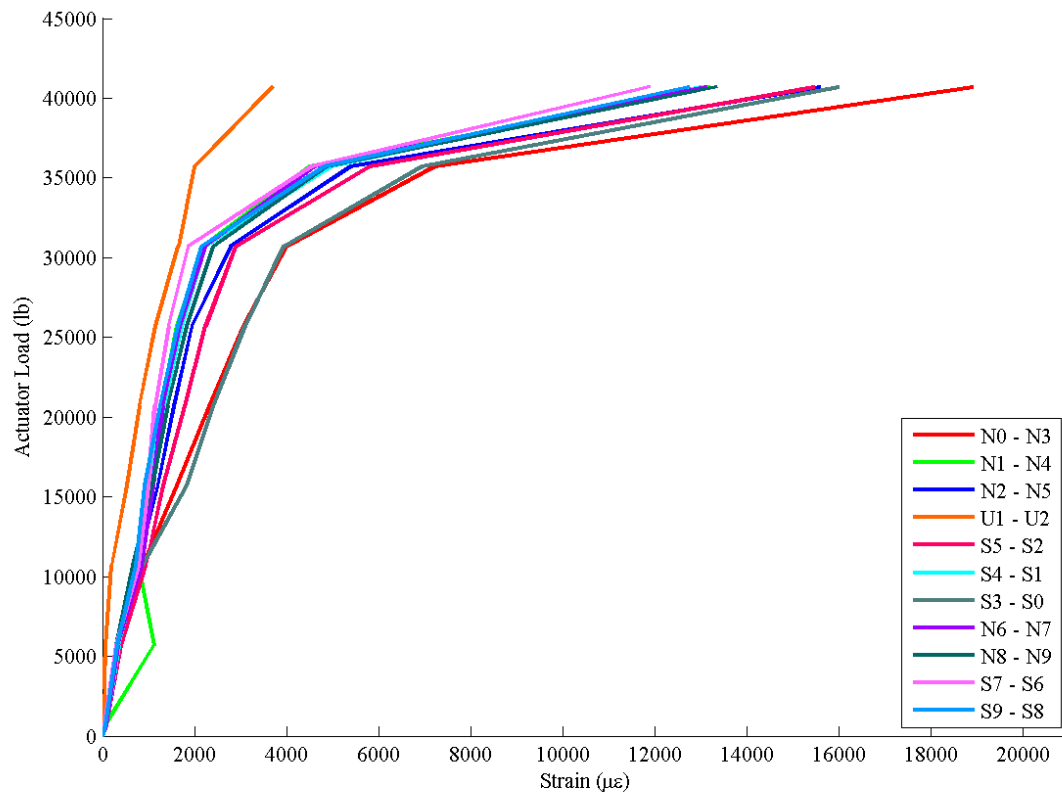


**Figure 68. Strain Variation Observed at the Top of the UHPC Pocket in U-6-7-I**